CESifo WORKING PAPERS

8347
2020

June 2020

The Social Cost of Contacts: Theory and Evidence for the COVID-19 Pandemic in Germany

Martin F. Quaas, Jasper N. Meya, Hanna Schenk, Björn Bos, Moritz A. Drupp, Till Requate

CESifo

Impressum:

CESifo Working Papers
ISSN 2364-1428 (electronic version)
Publisher and distributor: Munich Society for the Promotion of Economic Research - CESifo GmbH
The international platform of Ludwigs-Maximilians University's Center for Economic Studies and the ifo Institute
Poschingerstr. 5, 81679 Munich, Germany
Telephone +49 (0)89 2180-2740, Telefax +49 (0)89 2180-17845, email office@cesifo.de
Editor: Clemens Fuest
https://www.cesifo.org/en/wp
An electronic version of the paper may be downloaded
· from the SSRN website: www.SSRN.com
· from the RePEc website: www.RePEc.org
· from the CESifo website: https://www.cesifo.org/en/wp

CESifo *Working Paper No. 8347*

The Social Cost of Contacts:
Theory and Evidence for the COVID-19 Pandemic in Germany

Abstract

Building on the epidemiological SIR model we present an economic model with heterogeneous individuals deriving utility from social contacts creating infection risks. Focusing on social distancing of individuals susceptible to an infection we theoretically analyze the gap between private and social cost of contacts. To quantify this gap, we calibrate the model using German survey data on social distancing and impure altruism from the beginning of the COVID-19 pandemic. The optimal policy reduces contacts drastically in the beginning, to almost eradicate the epidemic, and keeps them at around a third of pre-pandemic levels with minor group-specific differences until a vaccine becomes tangible. Private protection efforts stabilize the epidemic in the laissez faire, though at a prevalence of infections much higher than optimal. Impure altruistic behaviour closes more than a quarter of the initial gap towards the social optimum. Our results suggests that private actions for self-protection and for the protection of others contribute substantially toward alleviating the problem of social cost.

JEL-Codes: I180, D620, D640.

Keywords: COVID-19, coronavirus, economic-epidemiology, private public good provision, impure altruism, uncertainty, SIR, social distancing, epidemic control.

*Martin F. Quaas**
German Centre for Integrative Biodiversity Research (iDiv), Halle-Jena-Leipzig / Germany
martin.quaas@idiv.de

Jasper N. Meya
German Centre for Integrative Biodiversity Research (iDiv), Halle-Jena-Leipzig / Germany
jasper.meya@idiv.de

Hanna Schenk
German Centre for Integrative Biodiversity Research (iDiv), Halle-Jena-Leipzig / Germany
hanna.schenk@idiv.de

Björn Bos
Department of Economics
University of Hamburg / Germany
bjoern.bos@uni-hamburg.de

Moritz A. Drupp
Department of Economics
University of Hamburg / Germany
moritz.drupp@uni-hamburg.de

Till Requate
Department of Economics
Kiel University / Germany
requate@bwl.uni-kiel.de

*corresponding author

May 29, 2020

1 Introduction

Reducing physical social contacts ('social distancing') has been a key measure to public disease control in the COVID-19 pandemic all over the world. While social distancing reduces the rates at which infected individuals infect others, it naturally comes at the cost of the forgone benefits of physical social contacts. As the COVID-19 global death toll has already surpassed 350,000 by the end of May, 2020, voluntary social distancing by risk averse and (impurely) altruistic individuals is a key ingredient for containing the virus. In general terms, the pandemic provides a natural experiment on private provision of a public good under uncertainty. In this paper, we investigate socially optimal contact reductions and to what extent contact reductions by risk averse and impurely altruisic individual susceptible to an infection comes close the social optimum.

To address this question, we extend the susceptible-infected-recovered (SIR) model of epidemiological dynamics (Kermack and McKendrick, 1927) by incorporating the behavior of heterogeneous, forward-looking individuals, differing in rates of infection, recovery, and mortality (implying heterogeneous basic reproductive numbers), and in their preferences. We focus on the behavior of susceptibles, taking the behavior of infected and recovered individuals as fixed. This focus allows us to contrast a private ('laissez-faire') Nash equilibrium with the Pareto-optimal social distancing policy targeting different population groups.

We provide analytical results on the gap between the private and social costs of contacts due to an infection externality. We show what drives the gap between purely selfish and socially optimal social distancing and that it declines with the degree of impure altruism. We identify two channels of how the severity of the disease, differing across socio-demographic groups, affects the optimal number of contacts. First, both the private and social costs of infection increase for subjects suffering more severely by the virus. Second, if an individual is less likely to infect others, which in our baseline model are those hit severely by the disease, this reduces the infection externality and allows for a larger number of contacts in the social optimum. Thus, according to theory, the overall effect is theoretically ambiguous.

To quantify the gap between private and socially optimal behaviour, we draw on a unique data set from a large, representative sample of around $3,500$ individuals in Germany at the beginning of the COVID-19 epidemic, and calibrate our model to official epidemiological statistics for Germany. Our survey elicits reported reductions in physical social contacts and the relative share of impurely altruistic motivation for social distancing, allowing us to derive the social cost of contacts without relying on estimates of the value of a statistical life (VSL) from other contexts, and to disentangle purely selfish from altruistic motivations. We conducted the survey in late March, when almost all Germans were still susceptible.

Our data collection period includes the introduction of the nation-wide contact ban, which is roughly equivalent to shelter-in-place policies in the US. While many social distancing policies aim at reducing mobility, the German contact ban focused specifically on reducing physical contacts, while leaving considerable room for voluntary behavior. This allows us to study private contributions to a public good for the case of social distancing, and to test for robustness concerning the role of regulation.[1] As the severity of COVID-19 differs with age and gender, our application to Germany distinguishes groups along these dimensions.

Our calibrated model provides the following results. First, the optimal social distancing policy reduces contacts drastically to bring infection numbers below 1 per $100,000$ individuals in the beginning, and stabilizes contacts at 32 to 37 percent of pre-pandemic levels to keep the basic reproduction number stable at one until a vaccine becomes tangible. Second, we find only small differences in social distancing across groups both in the laissez-faire equilibrium and in the social optimum. Our numerical analysis shows that more severely affected groups, in particular old men, can be slightly more lenient in reducing contacts, as they are less likely to infect others in our baseline model. A sensitivity analysis shows that this effect depends on the specific way how infected individuals infect others. Third, we find that the social cost of contacts exceeds the private cost by a factor of 5 at 10 infected per 100,000 individuals, and by a factor of 25 at 1 infected per 100,000. Fourth, we find that impure altruistic behaviour closes a substantial share of the gap towards the social optimum, with group-specific gap reductions ranging from 28 percent for old males to 32 percent for young females. Finally, we show that purely selfish protection reduces the number of contacts to a level that keeps the basic reproduction number at one, although the prevalence of the disease will be much higher than optimal. Accordingly, the death toll in the laissez faire Nash equilibrium is about 16 times higher than in the social optimum. Our finding that behavioral feedbacks will contain the spread of the virus also in the laissez-faire equilibrium without regulation of contacts is in line with general theory according to which self-protection can contribute to alleviating the problem of external effects (Bramoullé and Treich, 2009).

Our research adds to the rapidly growing literature on the economics of epidemics applied to the ongoing COVID-19 pandemic, which builds on earlier contributions on the economics of infectious diseases (e.g. Barrett 2003; Barrett and Hoel 2007; Fenichel et al. 2011; Fenichel 2013; Gersovitz and Hammer 2004; Gersovitz 2011; Greenwood et al. 2019; Morin et al. 2013; Rowthorn and Toxvaerd 2012). In particular, we extend upon Fenichel et al. (2011) regarding socially optimal and impure altruistic behavior with heterogeneous groups.

[1] Neither our survey data nor cell-phone data on movements indicate a clear effect of the contact ban; instead we find a continuous reduction of contacts highlighting the importance of voluntary action and softer regulations. For the US, Yan et al. (2020) find that households voluntarily reduce contacts in response to infection risk and that this voluntary behavior is partly crowded out by compulsory social distancing policies.

Our contribution of studying the stylized purely selfish and impure altruistic private versus social cost of contacts with heterogeneous groups is most closely related to recent work by Farboodi et al. (2020) and Acemoglu et al. (2020). Farboodi et al. (2020) build an optimal control model with a single agent to compare contacts for (i) a laissez-faire equilibrium, (ii) a social planner model that fully internalizing the externality, and (iii) a model with imperfect altruism. They calibrate their model based on the literature, including VSL estimates from Greenstone and Nigam (2020), and find that a laissez-faire equilibrium comes close to the decline in social activity as measured in US micro-data from SafeGraph. Their optimal policy, which accounts for the infection externality, would stabilize contacts at about 60 percent of pre-pandemic levels. In comparison to our work, they do not disentangle selfish and altruistic behavior and capture group heterogeneities. With a similar focus, Bethune and Korinek (2020) study the infection externalities and compare individual behavior with the social optimum in a SIR model calibrated using VSL estimates. For the US, they estimate the social cost of infections to be 3.5 fold higher than the private cost. They find that, in contrast to the laissez-faire equilibrium, the social planner would eradicate the disease, except if it's social cost is very small. Eichenbaum et al. (2020) use the SIR model in a representative agent setting to show that the equilibrium of selfish individuals is not Pareto efficient, as individuals take infection rates as given. Gerlagh (2020) studies the ratio of public and private benefits of reducing contacts in a simplified SIR model and finds that public benefits of optimal social distancing are an order of magnitude higher than the private benefits.

Acemoglu et al. (2020) extend the SIR model to heterogeneous groups and provide a closed-form solution of the dynamic model. Specifically, their 'Multi-Risk' model considers different age classes, which differ in their infection, hospitalization and mortality rates. In their calibration for the US, they specify parameters based on the literature and account for heterogeneity in some parameters across age groups, distinguishing young $(20-44)$, middle-aged $(45-65)$ and old (>65). They find that a targeted, group-specific social distancing policy reduces economic cost and lives lost compared to a undifferentiated policy. Building on this Multi-Risk SIR model, Gollier (2020) compares welfare effects of a 'suppression' policy, where the disease is eradicated, with a 'flatten the curve' policy, where infections are only kept below the capacities of the health systems. The model is calibrated for France, considering three age groups: young (0-18), middle-aged (19-64), and old (>65). Gerlagh (2020) considers heterogeneity in preferences about social contacts, health cost or transmission rates in a simplified SIR model. He shows that a group-specific optimal social distancing policy sets tighter distancing policies for elderly when based on health characteristics, but sets tighter distancing policies for the young when based on the transmission of the virus. Grimm et al. (2020) extend the SEIR model for, among others, heterogeneous infectiousness

parameters and solve it numerically with calibration from the literature for Germany.

Several other recent papers extend the SIR model to study social distancing behaviour and optimal policy response in the COVID-19 pandemic with different foci (e.g. Alvarez et al. 2020; Brotherhood et al. 2020; Chudik et al. 2020; Dasaratha 2020; Gonzalez-Eiras and Niepelt 2020; Jones et al. 2020; Pindyck 2020; Toxvaerd 2020). Of these, Alfaro et al. (2020) is most closely related to our paper. They use a homogenous SIR model to show that infected individuals internalise part of the infection externality due to altruistic preferences. Yet, their data does not allow for clearly disentangling to what extent altruistic motives narrow the gap between selfish and socially optimal behavior. Finally, our microeconomic focus leaves aside macroeconomic effects, such as fiscal consequences or income shocks related to the effects on trade or supply chains (see, e.g., Bodenstein et al., 2020; Coibion et al., 2020; Guerrieri et al., 2020; Rachel, 2020). In relation to income losses, which our surveyed households expect on average, our empirical strategy assumes that—as far as income is dependent on physical contacts—these income losses are captured by their individual reductions in contacts.

Finally our paper also relates to the literature on the private provision of a public good under uncertainty (e.g. Barrett and Dannenberg, 2014; Bramoullé and Treich, 2009; McBride, 2006; Tavoni et al., 2011; Quaas and Baumgärtner, 2008) and public good provision by impurely altruistic individuals (e.g. Andreoni, 1988, 1990; Goeree et al., 2002; Ottoni-Wilhelm et al., 2017), as it provides evidence for a more general theoretical hypothesis that uncertainty can help to alleviate the problem of external effects.

To the best of our knowledge, our paper is the first in this literature to (i) combine a heterogeneous, group-specific analytical model with survey data on adaptive behaviour to quantify the gap between the social and the private ('laissez-faire') optimum; (ii) estimate welfare effects based on empirical evidence, while disentangling purely selfish and altruistic components of social-distancing behavior. While so far most economic-epidemiological models are calibrated to US data, our application to Germany offers an interesting complementary case study, as an advanced economy that has managed the first month of the pandemic with relatively few deaths and relatively modest regulations.

The remainder of the paper is structured as follows. In Section 2 we introduce our economic-epidemiological model with heterogeneous groups (HetSIR), analytically characterise the Nash equilibrium under purely selfish behaviour, the utilitarian optimum and individual behaviour under imperfect altruism. We calibrate the full dynamic model in Section 3. For this, we estimate the economic parameters with survey data, calibrate epidemiological parameters and specify utility and behavioral parameters. We present our results in Section 4, test their robustness and consider extensions in Section 5. Section 6 concludes.

2 The economic-epidemiological model with heterogeneous groups (HetSIR)

2.1 Epidemiological dynamics

We draw on the canonical epidemological SIR model introduced by Kermack and McKendrick (1927), augmented by an additional equation of motion to include death (SIRD), and set up in discrete time. Total population in period t denoted by N_t splits up into susceptibles, S_t, infected and infectious, I_t, recovereds, R_t, and additionally we recor the number of deads D_t, such that $N_t = S_t + I_t + R_t = N_0 - (D_t - D_0)$. Recovereds are assumed to be immune.

We set up a heterogeneous model (HetSIR) allowing for different population groups j that differ in socio-demographic characteristics, for example in age and gender, and risk exposure. Considering this heterogeneity addresses limitations of the aggregate SIR model (Avery et al., 2020), and allows to study how incentives to choose frequencies of physical contacts with others c_{jt} differ with these characteristics.[2] Different frequencies of physical contacts result in heterogeneous effective infection rates. Individuals from different groups may also differ in their clinical course of the infection, resulting in heterogeneous fatality or recovery rates.

To keep the model tractable, we assume that individuals are homogeneous within a group and do not switch groups. The epidemiological dynamics how individuals of all groups change their health status are described by:

$$S_{j,t+1} = (1 - \mu_j)\, S_{jt} - \beta(c_{jt})\, \frac{\sum_l I_{lt}}{N_t}\, S_{jt}, \tag{1a}$$

$$I_{j,t+1} = (1 - \mu_j - \alpha_j - \gamma_j)\, I_{jt} + \beta(c_{jt})\, \frac{\sum_l I_{lt}}{N_t}\, S_{jt}, \tag{1b}$$

$$R_{j,t+1} = (1 - \mu_j)\, R_{jt} + \gamma_j\, I_{jt}, \tag{1c}$$

$$D_{j,t+1} = D_{jt} + \mu_j\, (S_{jt} + I_{jt} + R_{jt}) + \alpha_j\, I_{jt}, \tag{1d}$$

where $\beta(c_{jt})$ is the infection rate given the frequency of physical social contacts c_{jt} of susceptibles of group j.[3] Moreover, γ_j is the recovery rate, α_j denotes the rate at which infected individuals from group j die, and μ_j is the baseline, i.e., not corona-related, mortality rate for individuals of group j. According to this model, the probability of infections is proportional

[2] Likewise one can study protection efforts which would simply be modelled as inversely related to c_{jt}.

[3] In contrast to Farboodi et al. (2020) and Acemoglu et al. (2020) our focus is on the choice of contacts by susceptible individuals, and thus we keep behavior of the other groups fixed. Farboodi et al. (2020) differentiate contacts of susceptible versus infectious individuals, and self versus other contacts; Acemoglu et al. (2020) use a single parameter for the functional form of the infection term.

to the number of susceptibles, S_{jt}, which decreases over time. The infection probability is also proportional to the total number of infectious from any group, $I_t = \sum_j I_{jt}$. It increases until the peak of the pandemic and decreases thereafter. The basic reproduction number $\mathcal{R}_0$, i.e. the number of people infected by one individual on average, is defined as

$$\mathcal{R}_0 = \sum_j \frac{\beta(c_{j0})}{\mu_j + \alpha_j + \gamma_j} \frac{S_{j0}}{N_{j0}}, \tag{2}$$

calculated by the next generation method. Note that the basic reproduction number $\mathcal{R}_0$ is a function of contacts and can thus be reduced by social distancing policies. In a similar fashion, $\mathcal{R}_{j0} = \beta(c_{j0})/(\mu_j + \alpha_j + \gamma_j)$ are the group-specific basic reproduction numbers.

The current state of the epidemic is determined by the values of all state variables, i.e. the number of susceptibles, infected, and recovered from all groups. In the following, we also use $S_t{:=}\sum_j S_{jt}$, $I_t{:=}\sum_j I_{jt}$, $R_t{:=}\sum_j R_{jt}$ and $D_t{:=}\sum_j D_{jt}$ to denote the number of susceptibles, infected, recovered, and dead, aggregated over groups.

2.2 Equilibrium dynamics with private self-protection

A key interest of our paper is in the (forward-looking) choice of physical social contacts by susceptibles who we model as expected utility maximizers. For both the individuals and the society we assume a finite planning horizon of T weeks, where T is the expected time when a vaccination will become available. We assume that all individuals have the same expectation about T. After T weeks, group j individuals incur the present value utility level V_j^n, with superscript n denoting the no-epidemic situation.

Following the model of adaptive behavior suggested by Fenichel et al. (2011), each individual takes as given the time paths of S_{jt}, I_{jt}, and R_{jt}, for all groups j. We use $V_{jt}^h{:=}V_j^h(S_{1t}, S_{2t}, \ldots, I_{1t}, I_{2t}, \ldots, R_{1t}, R_{2t}, \ldots, t)$ to denote the value function for an individual of group j in health state $h \in \{s, i, r, d\}$ at time t, i.e. the expected present value of utility the individual attaches to reaching health state h. As usual, the model is solved backwards, starting with the final potential health states, recovered or dead.

The value function in the recovered health state r is given by

$$V_{jt}^r = u_j^r + \delta_j \left\{(1 - \mu_j)\, V_{j,t+1}^r + \mu_j\, V_j^d\right\}, \tag{3}$$

where $\delta_j \in (0, 1)$ denotes the utility discount factor, u_j^r the (Bernoulli) utility of recovereds, and V_j^d the present utility value of being dead. The term in curly brackets is the (von Neumann–Morgenstern) expected utility of either remaining in the recovered health state or non-corona related death. It directly follows that the value of being recovered V_j^r is

independent of the state of the epidemic and equal to

$$V_{jt}^r = \frac{u_j^r + \delta_j \, \mu_j \, V_j^d}{1 - \delta_j \, (1 - \mu_j)} \left(1 - (\delta_j \, (1 - \mu_j))^{T-t}\right) + V_j^n \, (\delta_j \, (1 - \mu_j))^{T-t} . \tag{4}$$

It is a weighted average between the infinite time-horizon value function for recovereds, the first fraction on the right-hand-side of (4), and the value of an individual in the no-epidemic situation, V_j^n. The weighting factor on the first component decreases, and the weighing factor on the second component increases, as the arrival time T of the vaccination approaches.

An infected individual from group j will recover with probability γ_j and die with probability $\alpha_j + \mu_j$, both of which are, by assumption, independent of the state of the epidemic, but vary with individual characteristics, such as age and general health conditions. In the following we use u_j^i to denote a group j individual's (Bernoulli) utility function in health state i. Using (4), the corresponding value function is determined by

$$V_{jt}^i = u_j^i + \delta_j \left\{ (1 - \mu_j - \gamma_j - \alpha_j) \, V_{j,t+1}^i + \gamma_j \, V_{jt}^r + (\mu_j + \alpha_j) \, V_j^d \right\}, \tag{5}$$

which is the sum of the utility of being infected plus the discounted expected utility of staying infected, recovering or dying.

Also V_{jt}^i is independent of the state of the epidemic, i.e. independent of the number of susceptible, infected, or recovered individuals. Solving (5), we obtain:

$$V_{jt}^i = \frac{u_j^i + \delta_j \, \gamma_j \, V_{jt}^r + \delta_j \, (\mu_j + \alpha_j) \, V_j^d}{1 - \delta_j \, (1 - \mu_j - \gamma_j - \alpha_j)} \left(1 - (\delta_j \, (1 - \mu_j - \alpha_j - \gamma_j))^{T-t}\right) + V_j^n \, (\delta_j \, (1 - \mu_j - \alpha_j - \gamma_j))^{T-t} . \tag{6}$$

Note that V_{jt}^i can be interpreted in terms of quality-adjusted life years. It is increasing in the quality of life, as measured by the utility levels u_j^i and u_j^r. The value V_{jt}^i is also monotonically increasing in the baseline survival rate $1-\mu_j$, and thus in the expected number of remaining life years absent the pandemic. Moreover, V_{jt}^i is monotonically decreasing with the 'severity' of the disease, as captured by the mortality rate α_j:

Proposition 1. *The value an individual attaches to an infection is monotonically decreasing in the COVID-19 mortality rate α_j, and monotonically increasing in the (Bernoulli) utility in the infected state, u_j^i.*

Proof. Noting that V_{jt}^r and V_j^d are independent of α_j, we get

$$\frac{dV_{jt}^i}{d\alpha_j} = -\delta_j \frac{u_i - (1-\delta_j)\, V_j^d + \delta_j\, \gamma_j\, \left(V_{jt}^r - V_j^d\right)}{\left(1 - \delta_j\, (1 - \mu_j - \gamma_j - \alpha_j)\right)^2}$$
$$- (T-t)\, \delta_j\, \left(\delta_j\, (1 - \mu_j - \alpha_j - \gamma_j)\right)^{T-t-1} \left(V_j^n - \frac{u_j^i + \delta_j\, \gamma_j\, V_{jt}^r + \delta_j\, (\mu_j + \alpha_j)\, V_j^d}{1 - \delta_j\, (1 - \mu_j - \gamma_j - \alpha_j)} \right) < 0, \tag{7}$$

as individuals prefer to be infected over being dead, expressed in momentary utility as $u_i > (1-\delta_j)\, V_j^d$. They prefer to be recovered over being dead, expressed in present values as $V_{jt}^r > V_j^d$, and they prefer to be in the situation with no epidemic compared to being infected, i.e. the last term in brackets on the right-hand-side of (7) is positive. The result on u_j^i follows immediately by differentiating (6) with respect to u_j^i. □

Differences in the Bernoulli utility functions, a susceptible individual attaches to the different health states, capture the effect of risk aversion. The more averse against health risk an individual is, the smaller will be u_j^i relative to the utility in the susceptible health state. Thus, the second statement in Proposition 1 shows that the present value an individual attaches to an infection is decreasing with the individual's (health-related) risk aversion.

Finally, we turn to the value of a susceptible individual, that is, in health state s. Recall that $\beta(c_{jt})\, I_t/N_t$ is the rate at which susceptibles get infected after having had physical contacts with infected. This infection rate increases with the frequency c_{jt} with which susceptible individuals have physical contacts with others, i.e. $\beta'(c_{jt}) > 0$. The value function for the individual in state s is determined by the Bellman equation:

$$V_{jt}^s = \max_{\{c_{jt}\}} \left[u_j^s(c_{jt}) + \delta_j \left\{ \left(1 - \mu_j - \beta(c_{jt})\, \frac{I_t}{N_t}\right) V_{j,t+1}^s + \beta(c_{jt})\, \frac{I_t}{N_t}\, V_{j,t+1}^i + \mu_j\, V_j^d \right\} \right], \tag{8}$$

with V_{jt}^i given in (6) and where utility u_j^s in state s is a concave function of contacts c_{jt}.

In the absence of regulation, and given S_{jt}, I_{jt}, and R_{jt}, for all groups j and at each point in time, a purely selfish individual chooses the frequency of physical social contacts, c_{jt}, to solve (8). The corresponding first-order condition is given by

$$u_j^{s\prime}(c_{jt}) = \delta_j\, \beta'(c_{jt})\, \frac{I_t}{N_t} \left(V_{j,t+1}^s - V_{j,t+1}^i \right). \tag{9}$$

An individual reduces physical social contacts such that her private marginal costs (lost marginal utility of c_{jt}) equals the expected marginal benefit in terms of extending the time enjoying utility V_{jt}^s rather than V_{jt}^i. The marginal benefit of reducing social contacts is the

discounted additional utility of staying susceptible weighted by the decreased rate of getting infected, $\beta'(c_{jt})\, I_t/N_t$, due to reductions in social contacts c_{jt}. If utility is concave in contacts, i.e. $u_j^{s\prime\prime}(c_{jt}) < 0$, a decrease of $u_j^{s\prime}(c_{jt})$ corresponds to an increase in c_{jt}. It directly follows from (9) that physical social contacts of susceptible individuals decrease with the current rate of infected in the population I_t/N_t. Moreover, physical social contacts of susceptible individuals c_{jt} decrease with the difference of an individual's present value utility of staying susceptible rather than becoming infected, i.e. $V_{j,t+1}^s - V_{j,t+1}^i$.

Whereas the individual present value of an infection V_{jt}^i is independent of the state of the epidemic, the individual present value in the susceptible state, V_{jt}^s, and the individually optimal number of contacts, c_{jt}, depend on the fraction of infected in the entire population, I_t/N_t. As epidemiological dynamics depend on the (aggregate) behavior of all members in society, also the dynamics of c_{jt} depends on the behavior of all others. Thus the choice of c_{jt} has to be determined as the equilibrium of a dynamic game. We consider the open-loop Nash equilibrium, where all individuals take as given the epidemiological dynamics, resulting from the behavior of all others. The Nash equilibrium is determined by the simultaneous solution, for all groups j, of the individual optimality condition (9), the Bellman equations (8) for V_{jt}^s; equation (6) determining V_{jt}^i, and the epidemiological dynamics (1).

2.3 Utilitarian optimum

We now study the socially optimal number of physical social contacts. The social objective is to maximize the sum of expected present value of individual utilities over the frequency of contacts of all individuals and at all time periods, i.e. the utilitarian welfare function. The function is based on the aggregation of unit comparable individual utility functions (Roemer, 1996). To construct unit comparable utility functions for the individuals, we normalize individual utility functions such that momentary utility prior to the COVID-19 pandemic is identical for all individuals, i.e. $\max_{c_j} u_j^s(c_j) = \max_{c_l} u_l^s(c_l)$ for all j, l. Given unit comparability, the utilitarian welfare function is a particularly appealing specification, as it is consistent with the assumptions that social preferences satisfy the von Neumann Morgenstern axioms (Harsanyi, 1955) and the Strong Pareto assumption, i.e., society prefers one allocation over another one if all individuals weakly prefer it and at least one individual strictly prefers it. As in Section 2.2, and in line with the standard approach in social welfare functions (Roemer, 1996), we only consider the purely selfish part of individual utility:

$$\hat{W} = \max_{\{c_{jt}\}} \sum_j \sum_{t=0}^{T} \delta_j^t \left(S_{jt}\, u_j^s(c_{jt}) + I_{jt}\, u_j^i + R_{jt}\, u_j^r + D_{jt}\, u_j^d \right), \tag{10}$$

subject to the epidemiological dynamics given by (1). Whereas each individual faces risks of changing their health status, at the societal level the epidemiological dynamics are deterministic. Thus, the problem (10) to find the utilitarian optimum is a standard deterministic dynamic optimization problem that can be solved by the Lagrangian method, using λ_{jt}^h as the Lagrangian multiplier for the number of individuals in health state $h \in \{s, i, r, d\}$ in period $t+1$. These Lagrangian multipliers have the interpretation of the social value, in units of utility, of an extra individual from group j in health state h. They are the social equivalent to the value $V_{j,t+1}^h$ an individual attaches to the health state h in period $t+1$.

The conditions characterizing the socially optimal physical social contacts $c_{jt}^\star$ under epidemiological dynamics can be written as follows, using $I_t = \sum_l I_{lt}$ and $\delta_j^t, S_{jt} > 0$:

$$u_j^{s\prime}(c_{jt}^\star) + \delta_j \, \beta'(c_{jt}^\star) \, \frac{I_t}{N_t} \, \left(\lambda_{jt}^i - \lambda_{jt}^s\right) = 0 \tag{11a}$$

$$u_j^s(c_{jt}^\star) - \lambda_{j,t-1}^s + \delta_j \, \lambda_{jt}^s + \delta_j \, \beta(c_{jt}^\star) \, \frac{I_t}{N_t} \, \left(\lambda_{jt}^i - \lambda_{jt}^s\right) + \delta_j \, \mu_j \, \left(\lambda_{jt}^d - \lambda_{jt}^s\right) = 0 \tag{11b}$$

$$u_j^i - \lambda_{j,t-1}^i + \delta_j \, \lambda_{jt}^i + \delta_j \, \gamma_j \, \left(\lambda_{jt}^r - \lambda_{jt}^i\right) + \delta_j \, (\mu_j + \alpha_j) \, \left(\lambda_{jt}^d - \lambda_{jt}^i\right) = \sum_l \, \delta_l \, \beta(c_{lt}^\star) \, \frac{S_{lt}}{N_t} \, \left(\lambda_{lt}^s - \lambda_{lt}^i\right) \tag{11c}$$

$$u_j^r - \lambda_{j,t-1}^r + \delta_j \, \lambda_{jt}^r + \delta_j \, \mu_j \, \left(\lambda_{jt}^d - \lambda_{jt}^r\right) = 0 \tag{11d}$$

$$u_j^d - \lambda_{j,t-1}^d + \delta_j \, \lambda_{jt}^d = 0, \tag{11e}$$

with transversality conditions $\lambda_{jT}^h = V_j^n$ for all $h \in \{s, i, r\}$.

Conditions (11a) and (11b) for the social optimum are formally equivalent to conditions (8) and (9) for the private optimum, except that the individual value of being in state s (or i) at time $t+1$, $V_{j,t+1}^s$ (or $V_{j,t+1}^i$), is replaced by the social value of an extra individual in state s (or i) at time t, λ_{jt}^s (or λ_{jt}^i). The calculus for determining the optimal number of physical social contacts is the same for the utilitarian planner as for an individual. The marginal utility of an extra contact is set equal to the marginal cost in terms of increased number of individuals becoming infected. The difference, however, is that the planner considers the social cost of one extra individual becoming infected, which is $\lambda_{jt}^s - \lambda_{jt}^i$, and different from the individual cost of becoming infected, $V_{jt}^s - V_{jt}^i$.

For the dead or recovered individuals, there is no difference between social and individual values, as being dead or recovered does not effect the health of others. The social value of an extra dead is constant over time, $\forall t : \lambda_{jt}^d = \lambda_{j,t-1}^d = V_j^d$, and we thus obtain from (11d):

$$\lambda_{jt}^r = V_{jt}^r = \frac{u_j^r + \delta_j \, \mu_j \, V_j^d}{1 - \delta_j \, (1 - \mu_j)} \, \left(1 - (\delta_j \, (1 - \mu_j))^{T-t}\right) + V_j^n \, (\delta_j \, (1 - \mu_j))^{T-t} \, . \tag{12}$$

The key difference between individual and social optimum is that (11c) differs from (5) in that the condition for the social optimum includes the effect of a change in the number of infected of type j on all susceptible individuals. Especially if there are many susceptible individuals relative to infected individuals, this can make a substantial difference. Inserting (12) and (6) in (11c) and solving establishes the following expression for the social value of an extra infected individual from group j:

Proposition 2. *The social cost of an infection in population group j at time t is given as the private cost of the infection minus the net present value of the infection externality on all others:*

$$\lambda_{jt}^{i} = V_{jt}^{i} - \sum_{\tau=t+1}^{T} \left(\delta_j \left(1-\mu_j-\alpha_j-\gamma_j\right)\right)^{\tau-(t+1)} \sum_{l} \delta_l \, \beta(c_{l\tau}^{\star}) \, \frac{S_{l\tau}}{N_\tau} \left(\lambda_{l\tau}^{s} - \lambda_{l\tau}^{i}\right), \qquad (13)$$

where V_{jt}^{i} is the individual value of being infected, given by (6); where $\delta_l \, \beta(c_{l\tau}^{\star}) \, \frac{S_{l\tau}}{N_\tau} \, (\lambda_{l\tau}^{s} - \lambda_{l\tau}^{i})$ is the current-value external effect of the infection on individuals of population group l at time τ and where $\delta_j \left(1-\mu_j-\alpha_j-\gamma_j\right)$ is the population group-specific discount factor.

The difference between the value society attaches to an additional infected individual and the value from the individual's perspective—the second term on the right-hand-side of (13)—is negative, since $\lambda_{l\tau}^{s} > \lambda_{l\tau}^{i}$. Society attaches a higher damage to an extra infection than the individual. In other words, the social cost of an additional infection is higher than the private cost. The reason is that getting infected has a negative external effect as it increases the probability of an infection for all susceptibles in society. The second term on the right-hand-side of (13) quantifies the negative external effect of physical social contacts, defined as the difference between the social cost and the private cost. It is the present value of the social costs of an extra infected individual for all individuals in society from now on until the vaccination arrives.

The severity of the disease for group j, as measured by the mortality rate α_j, does not directly enter condition (11b) governing the dynamics of λ_{jt}^{s}, and enters (13) via the individual value of getting infected, V_{jt}^{i} (cf. Proposition 1), and via the discount factor in the second term on the right-hand-side of (13). Focusing on the second effect, we establish:

Proposition 3. *For two groups j and j' of individuals that have the same individual value of getting infected, $V_{jt}^{i} = V_{j't}^{i}$ for all t, and have identical discount factors, baseline mortality and recovery rates, $\delta_j = \delta_{j'}$, $\mu_j = \mu_{j'}$ and $\gamma_j = \gamma_{j'}$, the social value of an extra infected is higher for the group with the higher mortality risk.*

Proof. Under the given conditions, the difference in the social values of an extra infected individual from the two groups j and l is

$$\lambda_{jt}^{i} - \lambda_{lt}^{i} = \sum_{\tau=t+1}^{T} \Bigg(\left(\delta_l \left(1 - \mu_l - \alpha_l - \gamma_l\right)\right)^{\tau-(t+1)} - \left(\delta_j \left(1 - \mu_j - \alpha_j - \gamma_j\right)\right)^{\tau-(t+1)} \Bigg) \delta_l \, \beta(c_{l\tau}^{\star}) \, \frac{S_{l\tau}}{N_\tau} \left(\lambda_{l\tau}^{s} - \lambda_{l\tau}^{i}\right), \quad (14)$$

which is positive if and only if $\mu_j + \alpha_j + \gamma_j > \mu_l + \alpha_l + \gamma_l$. □

Ceteris paribus, the more severely a group of individuals is affected by the disease, the lower is the risk that an extra infected from that group exerts on susceptibles from the same and other groups. Thus, society can more extensively rely on self-protection by individuals from relatively more affected groups. Similarly, ceteris paribus, the more quickly an individual recovers, i.e. the higher γ_j, the smaller is the size of the external effects.

In terms of the optimal absolute number of physical social contacts, the effect of α_j is theoretically ambiguous. The private value of self-protection increases with α_j (cf. Proposition 1), whereas the magnitude of the external effect decreases with α_j (cf. Proposition 3). Which of the two effects dominates depends in particular on the individual Bernoulli utility functions for the different health states. It is thus an empirical question which group should be more restrictive in terms of the number of physical social contacts.

For the empirical application, we utilize a property of the model that becomes obvious in (13): For determining the optimal social distancing policy, the regulator does not need to have detailed knowledge of the individual Bernoulli utility functions for the health states of being infected, recovered, or dead. All relevant information is contained in the individual present value of becoming infected, V_{jt}^{i}, and conditions (11d) and (11e) can be ignored, provided μ_j is small enough that it can be ignored in (11b). The only additional information that the regulator needs to have of the individual preferences are the utility discount factors δ_j and the momentary utility derived from physical social contacts, $u_j^s(c_{jt})$. Thus, we establish:

Proposition 4. *If $\mu_j = 0$ for all j, the first-best social distancing policy can be computed from information on epidemiological parameters and on*

- *individual present values of becoming infected, V_{jt}^{i};*
- *utility discount factors, δ_j; and*
- *momentary utilities derived from physical social contacts, $u_j^s(c_{jt})$.*

No separate information on individual Bernoulli utility functions for the health states $y \in \{i, r, d\}$ is required.

Given the information specified in Proposition 4, one has to solve the system of equations (1), (11a), (11b), and (13), along with initial conditions for the number of susceptibles, infected, and recovered from all groups of individuals, and transversality conditions.

2.4 Individual behavior under imperfect altruism

We think of a perfectly altruistic individual as one who puts herself in the shoes of the social planner, i.e. who chooses her individual contacts according to (11a), whereas a purely selfish individual would choose contacts according to (9), as derived in Section 2.2.

An imperfectly altruistic individual is modeled as a hybrid between the two extremes, and thus would choose her physical social contacts $\hat{c}_{jt}$ according to

$$u_j^{s\prime}(\hat{c}_{jt}) = \delta_j \, \beta'(\hat{c}_{jt}) \, \frac{I_t}{N_t} \left((1-\varphi_j) \, \left(V_{jt}^s - V_{jt}^i \right) + \varphi_j \, \left(\lambda_{jt}^s - \lambda_{jt}^i \right) \right), \tag{15}$$

where $\varphi_j \in [0,1]$ is the individual's degree of altruism between zero, for the purely selfish individual, and one, for the perfectly altruistic individual.

For a given degree of altruism, φ_j, we can use (9) and (11a) to alternatively write

$$u_j^{s\prime}(\hat{c}_{jt}) = (1-\varphi_j) \, u_j^{s\prime}(c_{jt}) + \varphi_j \, u_j^{s\prime}(c_{jt}^\star), \tag{16}$$

where c_{jt} ($c_{jt}^\star$) are the purely selfish individual (utilitarian optimal) contacts.

We further use ψ_j to denote the share of the marginal expected costs of social contacts that are due to the purely selfish motivation, that is, we write

$$u_j^{s\prime}(c_{jt}) = \psi_j \, u_j^{s\prime}(\hat{c}_{jt}). \tag{17}$$

The remaining fraction $1-\psi_j$ corresponds to the extra reduction effort the individual spends for others. In our calibration to Germany (Section 3), we use observations on $\hat{c}_{jt}$ and ψ_j in (17) to estimate the number of physical social contacts a respondent would have chosen for purely selfish reasons. We furthermore observe that there is a monotonic relationship between ψ_j and the degree of altruism:

$$\psi_j = \frac{u_j^{s\prime}(c_{jt})}{u_j^{s\prime}(\hat{c}_{jt})} = \frac{u_j^{s\prime}(c_{jt})}{u_j^{s\prime}(c_{jt}) + \varphi_j \, \left(u_j^{s\prime}(c_{jt}^\star) - u_j^{s\prime}(c_{jt}) \right)}. \tag{18}$$

The higher the degree of altruism, the lower is the share of marginal expected costs of social contacts that are due to the selfish motivation. For $\varphi_j = 0$, we have $\psi_j = 1$ and $\hat{c}_{jt} = c_{jt}$; for $\varphi_j = 1$, $\psi_j = u_j^{s\prime}(c_{jt})/u_j^{s\prime}(c_{jt}^\star)$, implying $\hat{c}_{jt} = c_{jt}^\star$.

3 Calibration for Germany

We are particularly interested in how behaviour of susceptible individuals depends on the differential risk of a severe illness. Hence, we consider four population groups based on age and gender. With regard to age, we differentiate between respondents younger than 60 years of age (young) and those with an age of at least 60 years (old) as this threshold is also commonly used to classify between epidemiological high- and low-risk groups. In total, we consider the four groups of young men, young women, old men, and old women.

3.1 Survey data

For the economic parameters we predominantly rely on survey data that we elicited from a representative sample of 3,501 Germans from March 20 to 27, 2020, and combine this with estimates on time preferences from the literature.[4] In Table 1, we report the main variables of interest for the overall sample as well as for each population group individually (for additional summary statistics please refer to Table 5 in the Appendix).[5]

To elicit behavioral responses and to quantify reductions in the number of physical social contacts (c_{jt}), we asked respondents: *"Compared to the same week last year, by what percentage have you reduced or increased your physical, social contacts this week?"*. In the survey, we defined *"physical, social contacts"* as situations in which the respondent came closer than two metres to others. We collected responses on a 15-point log-scale ranging from *"reduction to zero"* to *"increasing by 10%"* which corresponds to a range of c_{jt}, relative to normal, in the interval $[0; 1.1]$.[6] Converting the responses to actual values, the mean response corresponds to a frequency of physical social contacts of $\hat{c}_{jt} = 0.25$ relative to normal. At the same time, we observe some heterogeneity between population groups (see Table 1).

[4]The survey respondents are representative for the German population in terms of gender, age, education, and income. We excluded 112 respondents that answered the survey in less [more] than 3 [60] minutes due to concerns regarding fast-clicking or inattention as well as 3 respondents with a diverse gender as this population group would be too small for our analysis. We pre-registered the survey at the AEA RCT Registry (`https://doi.org/10.1257/rct.5573-1.1`) and provide further details on the study in the Appendix.

[5]Besides the main inputs to our model, the survey included, among others, questions to elicit expectations regarding income losses, and expectations of getting infected or getting into acute danger due to an infection, which we analyze in a companion paper (Bos et al., 2020). At the time of our data collection, respondents expected on average only slight reductions by 1 percent in their annual household income for 2020 relative to 2019. Regarding the expectations about infections and the severity of the disease, we find that around 38 percent expect to get infected with the coronavirus over the course of the pandemic. When examining group heterogeneity, we find in particular that the younger groups have a significantly higher expectation to get infected and to get slightly ill, while the older groups have a significantly higher expectation to get into acute danger once infected (see Table 1). Finally, we find that the majority of respondents in all groups state that they changed their behavior more than what has been required.

[6]The answer items were: *"reduction to zero, ..., reduction to one hundredth, ..., reduction to one tenth, ..., halving, .., reducing by 10%, ..., reducing by 1%, unchanged, increasing by 1%, ..., increasing by 10%"*.

Our survey provides some evidence that respondents behave in an imperfectly altruistic manner, as modeled in Section 2.4. From another question in the survey, we know that defense measures can only in part be attributed by pure selfish behavior.[7] We observe that respondents, on average, attach a weight of only $\psi_j = 52$ percent to protect themselves when considering private defense measures. Thus, a considerable share of the reduction in contacts is not attributable to pure selfish behavior, but is due to impure altruistic motives, relating to the protection of family members and close friends (with a mean weight of 30 percent), as well as to others (18 percent). Although the motivation to contribute to the public good does not differ across gender, respondents older than 60 years attach a significantly higher 'selfish' weight on themselves when considering defense efforts. While young women (men) attach a weight of 49.2 (50.1) percent on impure altruistic motives, this altruistic weight is only 45.0 (43.7) percent for old women (men). We explain in Section 3.3 how we use this information to specify the hypothetical benchmark case of pure selfish behavior.

Besides the intrinsic motivation to engage in defense measures, external factors like governmental regulations could also affect private defense measures and potentially crowd out some of the intrinsic motivation (see, e.g., Yan et al., 2020). We test for this by comparing differences in responses for those who participate in the survey before and after a contact ban for Germany has been announced on Sunday, March 22, 2020. While the announcement took place roughly in the middle of our data collection period, this leaves approximately half of the respondents unaffected by the contact ban, and at least some share of the week in question subject to regulation for the other half. We report the results of this analysis in Section 5.2, which indicates that the contact ban had no clear effect on both defense measures and impure-altruistic motives.

Second, to calibrate time preferences (δ_j), we rely on a mix of evidence from the literature and data from our survey. As far as we know, there is no study that directly elicits utility discount rates from individuals. The most common approach to estimate time preferences is to use incentivized 'money earlier or later' designs (see Cohen et al., 2020, for a recent summary). These approaches include a variety of elaborate designs trying to disentangle time preferences from utility curvature or to circumvent utility measurement altogether (see, e.g., Andreoni and Sprenger, 2012; Attema et al., 2016; Harrison et al., 2002). Annual time preference rates in these experiments on individual (financial) discount rates usually vary between 25 and 35 percent. For the German population, Dohmen et al. (2010) estimate a median estimate from an incentivized elicitation of time preferences that is right within

[7] In question no. 19 we ask: *"As far as you reduce physical, social contacts or take protective efforts such as intensive hand washing, in what proportions (in percentage points that sum up to 100%) do you do this in order to (i) Protect yourself and members of your household [x%]; (ii) Protect your family and close friends [y%]; Protect other people [100-x-y%]."*

Table 1: Descriptive statistics of relevant survey responses.

	All	Population Group							
		Young men (j=1)		Young women (j=2)		Old men (j=3)		Old women (j=4)	
Change in contacts	4.81	5.31	***	4.35	***	5.16	**	4.51	*
(15-point Likert scale)	(3.48)	(3.48)		(3.41)		(3.35)		(3.61	
Reason for defense efforts (in %)									
To protect me	51.96	49.89	***	50.76	*	56.31	***	55.00	***
	(21.75)	(22.26)		(20.74)		(21.83)		(22.14)	
To protect family & friends	30.03	29.94		31.14	**	28.87		28.58	*
	(15.90)	(16.33)		(15.36)		(16.53)		(15.37)	
To protect others	18.01	20.18	***	18.10		14.82	***	16.43	**
	(14.37)	(16.24)		(13.39)		(12.97)		(12.92)	
Expectations									
Expected income change	6.98	6.97		6.44	***	7.85	***	7.45	***
(15-point Likert scale)	(2.41)	(2.49)		(2.50)		(1.89)		(2.10)	
P(get infected) (in %)	38.10	41.29	***	40.16	***	32.33	***	31.78	***
	(22.40)	(23.33)		(23.15)		(19.27)		(18.74)	
P(get slightly ill) (in %)	50.65	54.00	***	53.42	***	44.76	***	42.34	***
	(21.71)	(21.75)		(21.57)		(20.10)		(20.26)	
P(get in acute danger) (in %)	34.65	31.74	***	30.48	***	42.52	***	43.27	***
	(20.88)	(19.62)		(18.92)		(21.58)		(22.73)	
Contacts wrt. regulation (in %)									
Less than required	0.07	0.10	***	0.06		0.07		0.03	***
	(0.26)	(0.29)		(0.25)		(0.25)		(0.17)	
According to regulations	0.30	0.34	***	0.32	*	0.21	***	0.24	**
	(0.46)	(0.47)		(0.47)		(0.41)		(0.43)	
More than required	0.63	0.57	***	0.62		0.72	***	0.73	***
	(0.48)	(0.50)		(0.49)		(0.45)		(0.44)	
General preferences									
Patience	8.11	8.12		8.23	**	8.06		7.81	***
	(2.12)	(2.08)		(2.10)		(2.15)		(2.22)	
Observations	3501	1137		1312		561		491	

Notes: The table shows mean values and standard deviations in parentheses. Change in contacts was elicited with a logarithmic Likert scale as described in the main text. Expected income changes from 2019 to 2020 were elicited using a 15-point Likert scale ranging from 1 (reduction to 10 percent) to 15 (tenfold increase) with a value of 8 representing unchanged income. Patience was elicited using the Likert scale question from Falk et al. (2018). Stars indicate the significance of the mean values to the average mean values of the other groups (t-tests). * $p < 0.1$, ** $p < 0.05$, *** $p < 0.01$

Table 2: Parameters of the HetSIR model for individuals in the respective population groups. All rates are in units of 1/week.

	All	Population group			
		Young men (j=1)	Young women (j=2)	Old men (j=3)	Old women (j=4)
μ_j	0.000235	0.000028	0.000016	0.000844	0.000721
α_j	0.0306	0.00285	0.000863	0.125	0.0849
β_0	2.16	2.16	2.16	2.16	2.16
γ_j	0.689	0.689	0.689	0.689	0.689
$\mathcal{R}_0$	3.00	3.12	3.13	2.65	2.79
IFR_j (%)	3.86	0.41	0.13	15.36	10.95

this interval.[8] In following our revealed preference approach, we rely on these best available estimates of individual utility discount rates, but note that these are orders of magnitudes higher as compared to social utility discount rates as used by governments or recommended by economic experts (Drupp et al., 2018). While our parsimonious survey did not include an incentivized measure of δ, we elicited preferences for patience using the 11-point Likert scale question from Falk et al. (2018), where a 1 indicates 'very impatient' and an 11 'very patient', to obtain an indication of potentially heterogeneous time preferences across our groups. For our four population groups, we find some heterogeneity in patience levels ranging from a high level of impatience for old women (7.81) to a low level for young women (8.23). We find no difference between young and old men (with patience levels of 8.12 and 8.06, respectively).

For our main calibration we take a central estimate from the literature and use a 30 percent annual discount rate, i.e. $\delta = 1.3^{-1/52} = 0.995$ per week. We show in Section 5.1 that our results are not sensitive to substantially different assumptions on time preference rates.

3.2 Calibration of epidemiological parameters

We calibrate group-specific estimates for the COVID-19 mortality rate, α_j, and the background mortality rate, μ_j. In the baseline calibration, we assume that the baseline infection rate, β_0, and the recovery rate, γ_j, is identical for all groups j. This means that differences in infection rates are captured exclusively by differences in social physical contacts between groups. We summarize our resulting group-specific epidemiological parameters in Table 2.

[8] Dohmen et al. (2010) use a representative sample of 500 Germans and employ a multiple price list offering 100 Euros 'today' versus amounts that increased from 100 to 156.2 Euros in 12 months. Assuming locally linear utility and semiannual compounding, they compute a median discount rate of 27.5 to 30 percent, which is likely a conservative estimate due to a large fraction of respondents that never switched.

Our estimate for γ_j is obtained from the time period that an infected individual is infectious, based on He et al. (2020). This study analyzes viral load over time and finds that infectiousness starts two days before symptom onset and declines quickly thereafter, such that the density was less than 5 percent on day 4. We thus assume an infectious period of 6 days, which corresponds to an exponential recovery rate of 1/6 days in a continuous time model. In our discrete time model the recovery rate is $\gamma_j = 1 - e^{-7/6}$ per week.

The background mortality rates, μ_j, are computed based on official mortality tables of the Federal Statistical Office Germany (2020) for the most recent years 2016/2018. We estimate COVID-19 mortality rate α_j for each population group j as follows:[9] We use the daily number of new infections and new deaths in Germany reported by the Robert Koch Institut (2020b)[10] and aggregate them to the weekly level. We use (1) and replace $\beta(c_{jt}) \frac{\sum_l I_{lt}}{N_t} S_{jt}$ and $\alpha_j I_{jt}$ with the time series of reported new infections $\Delta I_{j,t+1}$ and new deaths $\Delta D_{j,t+1}$ respectively, and assume $\mu_j = 0$ as natural mortality is negligible on a weekly time scale (cf. Table 2). We suppose $I_{j,1} = 0$, since the estimation relies on data $\Delta I_{j,t}$, making $I_{j,1}$ unimportant and because reported cases in January and early February were probably still affected by imported cases (Pinotti et al., 2020; Rothe et al., 2020). We then estimate α_j by

$$\min_{\{\alpha_j\}} \sum_{j=1}^{4} \sum_{t=1}^{15} \left(I_{j,t}\, \alpha_j - \Delta D_{j,t+1} \right)^2 , \tag{19}$$

subject to $I_{j,t+1} = (1-\gamma)\, I_{jt} + \Delta I_{j,t+1} - \Delta D_{j,t+1}$. This gives α_j and $\text{IFR}_j = \frac{\alpha_j}{\alpha_j+\gamma+\mu_j}$ as shown in Table 2.[11] (Baud et al., 2020). The estimated mean IFR of 3.86 percent for the German population is close to the fatality rates reported by the WHO (Baud et al., 2020).

The initial basic reproduction number $\mathcal{R}_0$ was estimated to be between 2 and 3 (Boldog et al., 2020; Ferretti et al., 2020; an der Heiden and Buchholz, 2020; Read et al., 2020), although higher values with a range of 3 to 12 (Maier and Brockmann, 2020) or up to 14.8 (Rocklöv et al., 2020) have been suggested. We calibrate our model to the more conservative and widely accepted value of $\mathcal{R}_0 = 3$ for the German population during the initial phase of the pandemic. Using the weighted mean rates of recovery and mortality, we estimate the

[9] A number of studies have compared mean case fatalities across countries (Dorigatti et al., 2020) or corrected values for time lags in symptom onset, case detection, death and presumed number of unknown cases (Famulare, 2020), but fatality estimates remain uncertain (Dowd et al., 2020; Li et al., 2020).

[10] The Robert Koch Institute, supervised by the German Federal Ministry of Health, is responsible for a continuous health monitoring and reports officially confirmed data on cumulative incidence and deaths (corresponding to $I + R + D$ in our model), and for the daily number of new infections (I) and deaths (D). Here, we consider the time period from January 6 to April 26, 2020 (calendar weeks $1 - 16$).

[11] Targeting fatality by age, Verity et al. (2020) find infection fatality ratios (IFR) of 0.145% (< 60) and 3.28% (≥ 60) and 0.657% overall. Note, that the age-group specific mortality rates employed by Acemoglu et al. (2020) also go back to this source.

infection rate $\beta_0 = 2.16$ at the beginning of the epidemic. Assuming an equal infection rate across groups at the start of the pandemic, we then calculate the group-specific $\mathcal{R}_0$ values.

3.3 Specification of utility and behavioral parameters

We assume that individuals have no systematic differences in their preferences over physical social contacts. By comparing the reported number of family members and friends between population groups, we can indirectly test this assumption for our survey data. While the number ranges between 13.76 (old women) and 14.55 (old men), differences across population groups are not significant. This provides evidence that the motivation to get in contact is homogeneous across our four population groups. We specify the utility function as

$$u_j^s(c_{jt}) = \frac{1}{1-\varepsilon}\left(c_{jt}^{\varepsilon} - \varepsilon\, c_{jt}\right). \tag{20}$$

This normalizes the 'normal', i.e. utility-maximizing, number of contacts to $c_{jt}^0 = 1$, and the maximum of utility to one, $u_j(1) = 1$, both independent of the specification of ε. For $c_{jt} < 1$, the specification of ε has an effect on the marginal utility of social contacts, however. The smaller ε, the higher marginal utility, i.e. the more strongly an individual wants to maintain at least some physical social contacts. In particular, for $\varepsilon > 1$, marginal utility is bounded for $c_{jt} \to 0$, whereas it is infinite for $\varepsilon \leq 1$ when $c_{jt} \to 0$. We specify a value moderately below one, i.e. $\varepsilon = 0.7$.[12]

To estimate c_{jt} for the period of the survey, we use reported changes in the number of physical social contacts in the past week (variable "Change in contacts", see Table 1). We map the original responses, recorded on a 15-point Likert scale ranging from "reduction to zero" to "increase by 10%" (see Footnote 6 for the full specification), to numerical values, interpolating the non-specified values. We further use the reasons for defense efforts (variable "To protect me", see Table 1) as an estimate for ψ defined in (17). From this we estimate the number of contacts a respondent would have chosen for purely selfish reasons as

$$c_{j0} = \left(1 + \psi_j\,\left(\hat{c}_{j0}^{\varepsilon} - 1\right)\right)^{\frac{1}{\varepsilon}}. \tag{21}$$

The observations for $\hat{c}_{j0}$ and the estimates for the choice of physical social contacts under purely selfish behavior c_{j0} are shown in Figure 1. For $\hat{c}_{j0}$, i.e. the observed imperfect altruistic behavior, the mean is 0.25 and for c_{j0}, i.e. the estimated purely selfish behaviour, the mean

[12]The results are robust against alternative specifications of ε, except if one specifies a value $\varepsilon > 1$. For a specification $\varepsilon > 1$, marginal utility of physical social contacts is bounded, and a complete lockdown of contacts, $c_{jt} = 0$, becomes optimal.

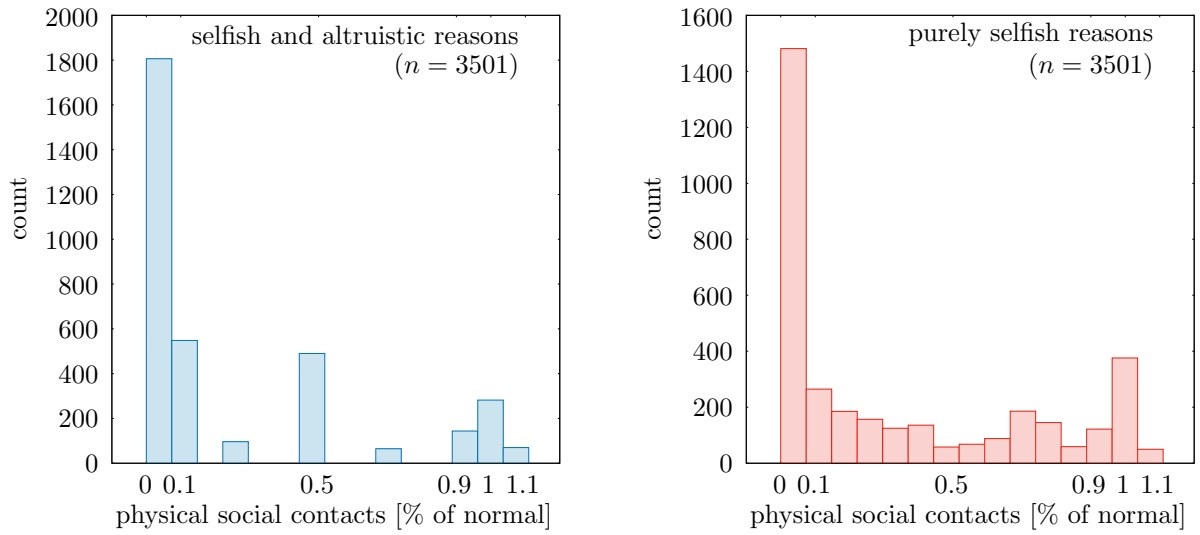

Figure 1: Histograms of surveyed impure altruistic physical social contacts (left), and estimated contacts under purely selfish behavior (right) compared to normal.

is 0.33. Mean reductions are thus to about a third of normal and reductions are more pronounced for altruistic behaviour. We use this estimated behavior to calculate the individual present value of getting infected, V^i_{jt}. To this end, we approximate the dynamic expectations under which the susceptible individual decides on physical social contacts given in (9) by a quasi-steady state, where I_{jt}, S_{jt}, and N_t are constant. Whereas this is only an approximation of the epidemiological dynamics, our survey data was collected during a phase where the number of infected individuals was by and large constant in Germany (see Figure 2).

Under the assumption that I_{jt}, S_{jt}, and N_t are fixed at their initial ($t = 0$) levels I_{j0}, S_{j0}, and N_0, we obtain the following private cost of a susceptible individual from group j becoming infected (by solving (8) for V^s_j and subtracting both sides of the equation by V^i_j):

$$V^s_{j0} - V^i_{j0} = \frac{u^s_j(c_{j0}) - (1 - \delta_j\,(1 - \mu_j))\,V^i_{j0}}{1 - \delta_j\,\left(1 - \mu_j - \beta(c_{j0})\,\frac{I_0}{N_0}\right)}. \tag{22}$$

Using the assumption of constant V^s_{jt} in (9), we get the following first-order condition for the individually optimal physical social contacts:

$$u^{s\prime}_j(c_{j0}) = \delta_j\,\beta'(c_{j0})\,\frac{I_0}{N_0}\left(V^s_{j0} - V^i_{j0}\right) \overset{(22)}{=} \delta_j\,\beta'(c_{j0})\,\frac{I_0}{N_0}\,\frac{u^s_j(c_{j0}) - (1 - \delta_j\,(1 - \mu_j))\,V^i_{j0}}{1 - \delta_j\,\left(1 - \mu_j - \beta(c_{j0})\,\frac{I_0}{N_0}\right)}. \tag{23}$$

For the remainder we follow Fenichel et al. (2011) by specifying $\beta(c_j) = \beta_0\,c_j$, which means that the probability of getting infected is proportional to the number of physical social

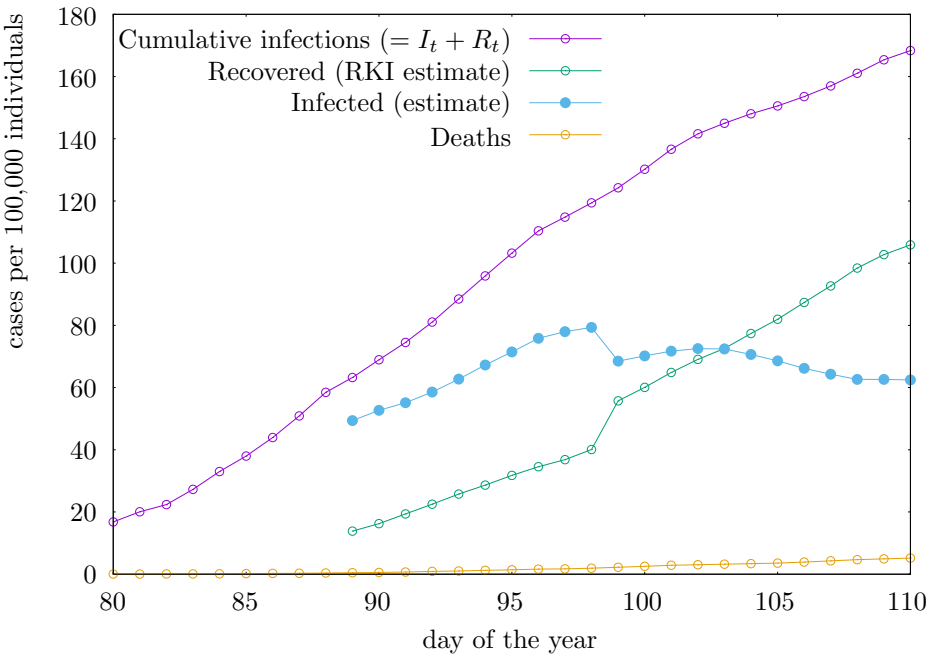

Figure 2: Dynamics of the COVID-19 pandemic in Germany in spring 2020, based on data from Robert Koch Institut (2020a). Cumulative infections and deaths are officially recorded, and the number of recovered is estimated by the Robert Koch Institute. We estimate the number of infected as the difference between cumulative cases and the estimated number of recovered. Our survey was conducted from calendar day 80 (March 20) to 87 (March 27).

contacts. Using individual utility in (20), as well as $\beta(c_j) = \beta_0\, c_j$ in (23) and rearranging, we obtain the individual present value of (dis-)utility of being infected ('private cost'):

$$V^i_{j0} = \frac{1}{1-\delta_j\,(1-\mu_j)}\left(c^{\varepsilon}_{j0} - \frac{\varepsilon}{1-\varepsilon}\,\frac{1-\delta_j\,(1-\mu_j)}{\delta_j\,\beta_0\,\frac{I_0}{N_0}}\,c^{\varepsilon-1}_{j0} + \frac{\varepsilon}{1-\varepsilon}\,\frac{1-\delta_j\,(1-\mu_j)}{\delta_j\,\beta_0\,\frac{I_0}{N_0}}\right). \tag{24}$$

We calibrate these values for the four groups based on the estimated individual choice of physical social contacts (see Figure 1) and the epidemiological parameters in Table 2.

Table 3: Estimates for individual present values of getting infected for the four groups, V^i_{j0}.

	Young men (j=1)	Young women (j=2)	Old men (j=3)	Old women (j=4)
Mean	-5,780	-7,117	-6,360	-7,522
SD	5,201	5,480	5,840	6,113
Median	-3,620	-3,991	-3,631	-6,072

Results are reported in Table 3. Generally we observe substantial heterogeneity of values within population groups, indicated by relatively large standard deviations. Moreover, distributions are skewed, as for most groups the (absolute value) median is much larger (smaller) than the mean. The mean values show patterns that are in line with our theory. As stated in Proposition 1 the individual damage of an infection should increase with the COVID-19 mortality risk. Consistent with the pattern of COVID-19 mortality rates (cf. Table 2), we find that the individual cost of being infected is larger for old than for young men and it is larger for old than for young women. Proposition 1 also states that the individual damage of an infection increases if u_j^i is small, which is the case especially for risk averse individuals. We find that the expected dis-utility of an infection is larger for women than for men, which is consistent with the observation that women are less willing to take health risks than men.

4 Results

We present quantitative results for Germany in three steps. First, we focus on the utilitarian optimum, as studied in Section 2.3. Here, we compute socially optimal epidemiological dynamics starting at the initial infection rates mid March, i.e. at the time of our survey, and then vary initial infection rates to study how socially optimal frequency of physical social contacts depends on the number of infected. Second, we compare these results to equilibrium dynamics with purely selfish individuals, as studied in Section 2.2. Finally, we also consider the social distancing behavior of imperfectly altruistic individuals, as modeled in Section 2.4. We implement our dynamic optimization HetSIR model, and the solution of equilibrium dynamics, in the state-of-the art nonlinear programming solver Knitro with AMPL (Byrd et al., 1999, 2006). Programming codes are provided in the Appendix.

4.1 Utilitarian optimum

Figure 3 shows the socially optimal epidemiological dynamics, starting at the initial infection rates in Germany in mid March 2020, and the corresponding social distancing policy. Infection numbers follow a U-shaped pattern. It is optimal to drastically reduce infection numbers at the beginning, so that the disease is close to eradicated, with less than one infected per $100,000$ individuals (cf. Figure 3, left panel).

Infection numbers are kept below one infected per $100,000$ individuals until a few weeks before the vaccine arrives. To attain this optimal trajectory, contacts are drastically reduced initially compared to pre-pandemic numbers, and during the quasi-steady state with minimal infection numbers they are kept stable between 32 and 37 percent (see Figure 3, right panel).

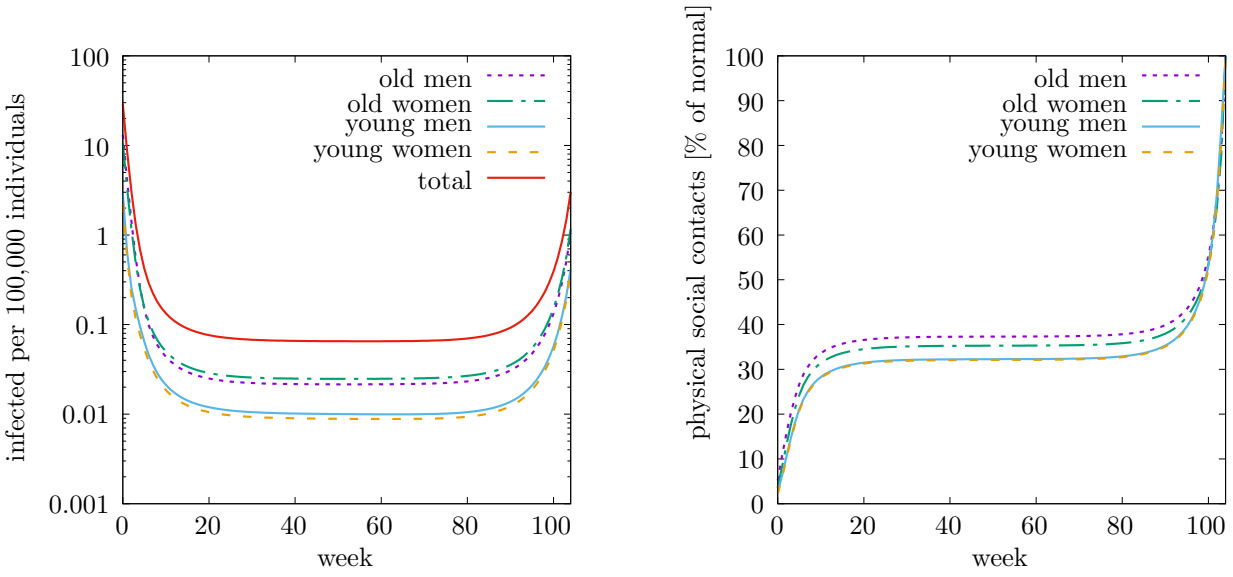

Figure 3: Dynamic optimization results. Parameter values as specified in the main text. We assume a planning horizon until a vaccination will become available of 104 weeks.

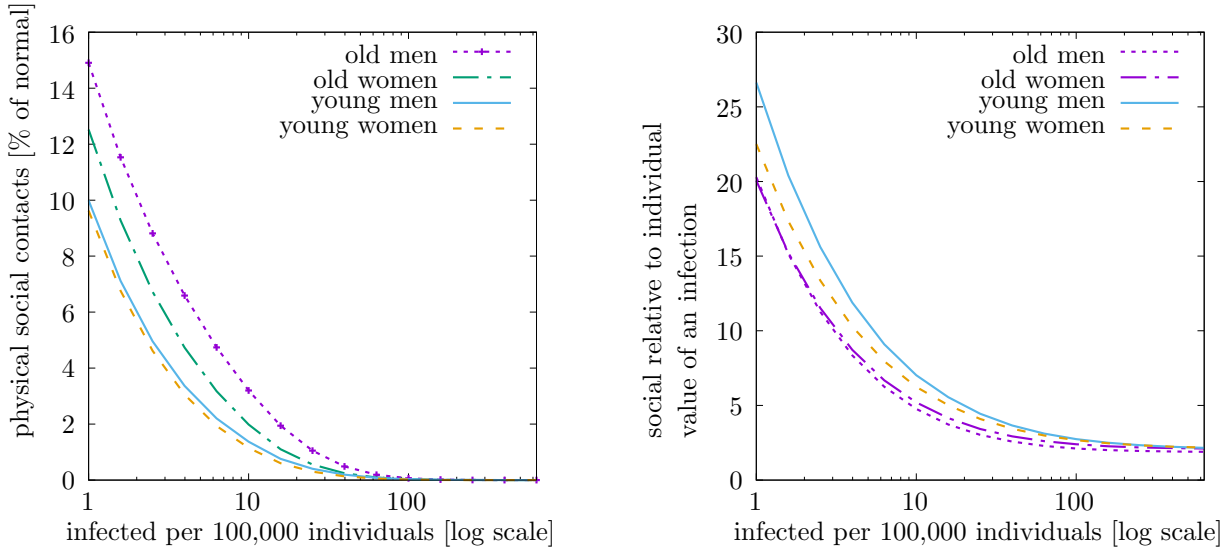

Figure 4: Optimal social distancing policy (left panel) and social cost relative to private cost of infection, λ^i_{jt}/V^i_{jt} (right panel) as a function of current infected. Parameter values as specified in the main text.

These values correspond to a basic reproduction rate of one, $\mathcal{R}_{j0} = 1$, i.e. one infected, on average, infects another individual. Using parameter values from Table 2 in equation (2), we obtain that the group-specific basic reproduction rate would be equal to one for the epidemiological parameters of young women or men if $\bar{c}_{1t} = \bar{c}_{2t} = 32$ percent, old men if $\bar{c}_{3t} = 37$ percent, or old women if $\bar{c}_{4t} = 35$ percent (the bar indicating the quasi steady state).

Contact allocations to specific groups show the largest differences in the phase of stabilisation (the 'new normal'), where old men are allowed to have the largest share of their normal contacts while young men and women face the largest contact reductions. This shows that differentiation of socially optimal distancing policy across groups is driven to a greater extent by the effect that older infected individuals, who tend to be more seriously hit by COVID-19, impose a lower risk on others (cf. Proposition 3) than by the effect that the expected present value of an infection is larger for these individuals (cf. Proposition 1). However, the differences between the groups are only in the range of single-digit percentage points and only of second order compared to overall contact reductions.

A question of particular interest is, how the socially optimal distancing policy depends on the initial number of infected. The left panel of Figure 4 shows that the optimal social distancing policy is a decreasing, convex function of current infection numbers. Already at one infected per $100,000$ individuals it is optimal to reduce physical social contacts to 10 to 15 percent of the level prior to the pandemic. At 10 infected per $100,000$ individuals contacts are reduced to 1.5 to 3.5 percent and at around 100 infected per $100,000$ individuals a complete lockdown is optimal.[13] Irrespective of the infection numbers, a utilitarian social planner would reduce the contacts of the young women and young men more than of the old women and old men, with the maximum difference in group-specific contact reductions being less than six percentage points. Note again, that differences in contact reduction between population groups are only of second order importance relative to the contact reductions over the pre-pandemic level, with the first order effect being the response to infection numbers.

Social costs relative to private costs, λ^i_{jt}/V^i_{jt}, are particularly high at low infection numbers (cf. Figure 4, right panel). At one infected per $100,000$ individuals the social cost is 20 to 27 times higher than the private cost. The ratio of social relative to the private cost is decreasing with current infection numbers, reflecting that the individual risk of an infection increases relative to the size of the external effect. This shows that higher the private risk, the more would risk-averse, rational individuals contribute to the public good of preventing the epidemic from spreading. To study this in more detail, we next compare equilibrium dynamics with purely selfish individuals to the utilitarian optimum.

[13] It is thus not optimal in our model to stop the pandemic by 'herd immunity', highlighting the importance of vaccines to minimise the time and social cost of epidemics.

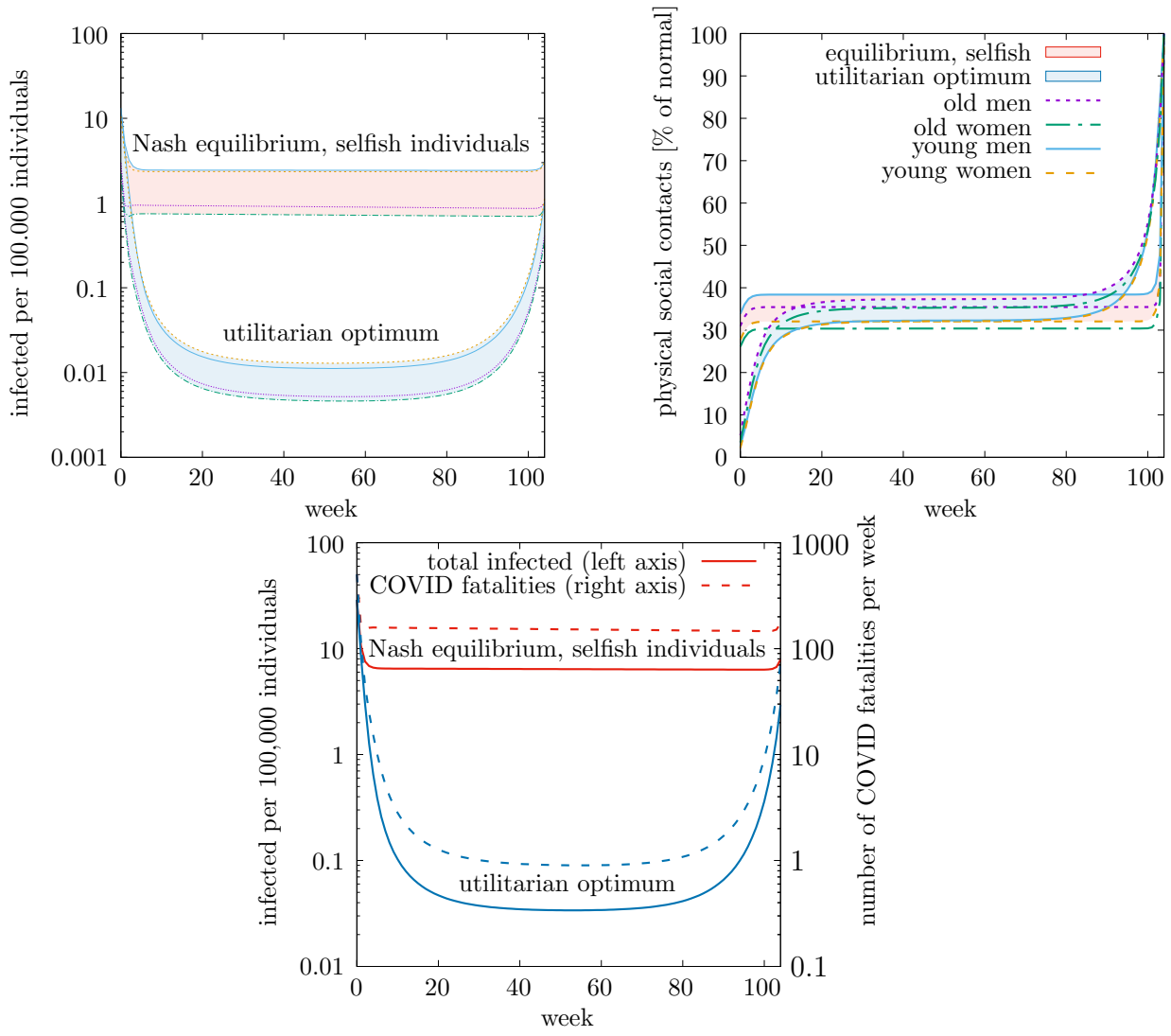

Figure 5: Epidemiological dynamics and individually optimal physical social contacts in Nash equilibrium of purely selfish individuals and under optimal social distancing policy (optimal dynamics as shown in Figure 3). Parameter values as specified in the main text.

4.2 Equilibrium dynamics with purely selfish individuals versus utilitarian optimum

Figure 5 compares the epidemiological dynamics (infected per 100,000 individuals, top left panel) and contacts (as percent of normal) for (a) the open-loop Nash equilibrium of purely selfish individuals and (b) the utilitarian optimum, i.e. the same as shown in Figure 3. In Nash equilibrium, the reduction in contacts is initially much smaller than optimal. Also in Nash equilibrium a quasi-steady state is reached, and contacts are reduced to the levels between 32 to 37 percent that keep the basic reproduction rate of the epidemic at one. This suggests that the selfish interest of rational, risk averse individuals to protect themselves from the disease may be sufficient to contain the virus. However, infection numbers in the quasi steady state differ by two orders of magnitude in the equilibrium and in the social optimum. As a result, much more individuals die from COVID-19 in the Nash equilibrium than in the optimum (Figure 5, bottom panel). Whereas in the utilitarian optimum, the total number of COVID-19 fatalities is 1,009 individuals, sixteen times more (16,352) individuals die from the disease in the Nash equilibrium with selfish individuals over the period of two years. Regarding differences across groups (Figure 5, top right panel), in Nash equilibrium, young men have most contacts, followed by old men, following the individual valuation of an infection, as shown in Proposition 1. The effect that more individuals who are more severely affected by the disease impose less risks on others, which plays the more important role in the social optimum (cf. Section 4.1), is irrelevant for equilibrium dynamics.

4.3 Social distancing behavior of imperfectly altruistic individuals versus selfish individuals versus utilitarian optimum

Table 4 compares the contact reductions at the beginning of the pandemic for three scenarios: The Nash equilibrium with purely selfish individuals, the Nash equilibrium with imperfectly altruistic individuals, and the utilitarian optimum. Selfish individuals would reduce their contacts already to between 29 percent (young women) and 40 percent (young men) of pre-pandemic levels. Altruistic behaviour, as observed in the survey, leads to even stronger contact reductions ranging, down to between 21 percent (young women) and 29 percent (young men). This closes the gap between contact reductions in the social optimum and the purely selfish Nash equilibrium by around 30 percent.

Figure 6 compares the number of contacts for a varying numbers of infected per 100,000 individuals for the same three scenarios. The comparison shows that the difference between equilibrium and optimal distancing becomes small in absolute numbers if the number of infected gets large, as the substantial individual risk of infections is then sufficient to spur

Table 4: Number of physical social contacts (all in % of normal) in the different scenarios (for initial conditions as in Figure 3; mid March in Germany) and degree of altruism (in %).

		Young men (1)	Young women (2)	Old men (3)	Old women (4)
Physical social contacts					
utilitarian optimum	$c^\star_{j0}$	2.59	2.22	5.22	3.51
selfish laissez-faire	c_{j0}	40.00	29.27	36.82	30.70
altruistic (observed)	$\hat{c}_{j0}$	29.17	20.73	27.30	22.77
altruistic contribution	$\frac{c_{j0}-\hat{c}_{j0}}{c_{j0}-c^\star_{j0}}$	28.95	31.57	30.31	29.17
degree of altruism	φ_j	7.80	9.34	11.78	10.23

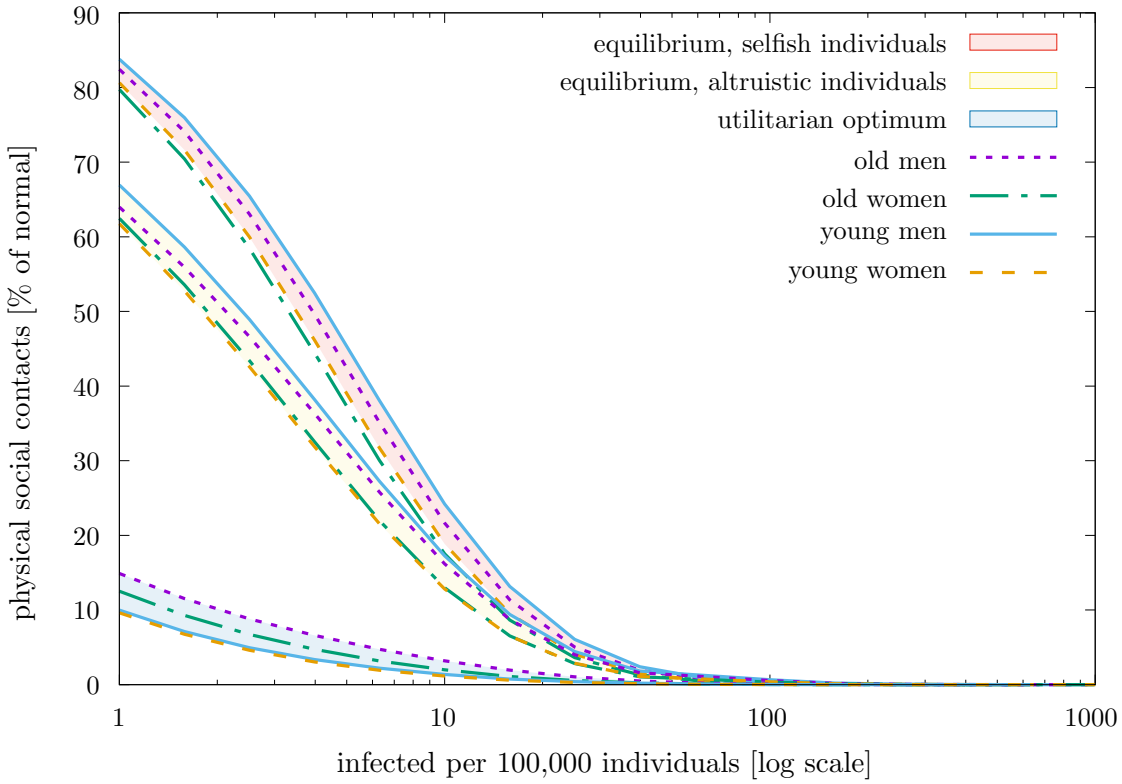

Figure 6: Comparison of physical social contacts (% of normal) in the Nash equilibrium with purely selfish individuals, in the Nash equilibrium with imperfectly altruistic individuals (actual), and in the utilitarian optimum.

private contributions to the public good by risk-averse individuals. The difference between the frequency of physical contacts between the equilibrium, both with selfish and with imperfectly altruistic individuals, increases considerably as the number of infected decreases. In other words, policy intervention is particularly necessary when there are few infected individuals, whereas rational individuals will sufficiently self-protect and thus voluntarily contribute to the public good if the number of infected individuals is already large.

5 Robustness checks and potential extensions

We perform a number of checks to study the sensitivity of our results to key parameters, examine whether the contact ban has altered the voluntary reductions in contacts, and discuss how results might change with possible model extensions.

5.1 Sensitivity analysis

We begin with a detailed sensitivity analysis regarding epidemiological parameters, discount rates or the time until a vaccine arrives. Figure 7 shows the results on the optimal dynamics in terms of the number of physical social contacts.

We first focus on the sensitivity regarding epidemiological parameters. In our baseline calibration, the effective time an infected individual can infect others decreases with mortality rate. We interpret this more generally as the effect that an individual hit severely by COVID-19 is less likely to infect others, also because severely infected individuals are detected earlier, are hospitalised or self-quarantined and therefore their effective infectious time is lower. Yet, it may also be that less severely affected individuals recover more quickly from the disease. One possible specification capturing this effect is to set $\alpha_j + \gamma_j$ constant across individuals. The top left panel of Figure 7 shows the results from this model specification. The main effect is that differences across groups in the socially optimal number of contacts are negligible in this alternative calibration. This shows that the results how to optimally differentiate social distancing policies across individuals depend on the exact way how individuals are affected by COVID-19 and how this translates into infection risks for others. The first-order effects of optimal social distancing, which are similar across groups, are robust, however.

Second, we study sensitivity with respect to preference parameters. Our baseline calibration assumes a weekly utility discount rate of 0.5 percent, corresponding to an annual discount rate of around 30 percent. We find, however, that the results are very robust against alternative specifications of the discount rate. Even for a very high discount rate of 5 percent per week, the general pattern of optimal dynamics remain similar, except that the

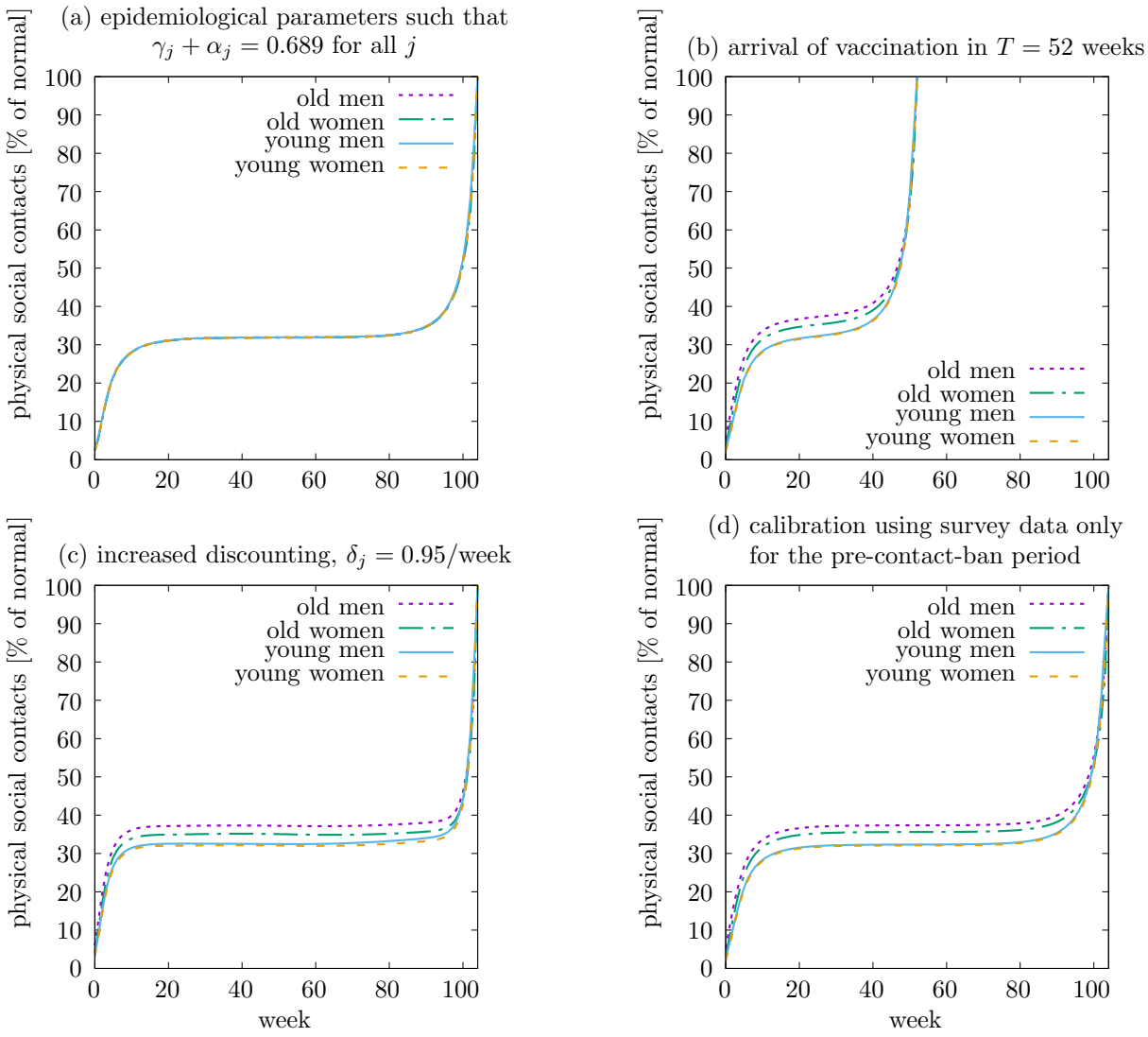

Figure 7: Results of the sensitivity analysis on the time path of physical social contacts in the utilitarian optimum. Panel (a), top left: the recovery rates for the three groups have been adjusted such that $\gamma_j + \alpha_j$ is identical for all groups and equal to the value of γ_j in the baseline calibration; for panel (b), top right, the time horizon is shortened to $T = 52$ weeks; for panel (c), bottom left, the discount rate is increased to $\delta_j = 0.95$ per week; for panel (d), bottom right, the model is calibrated using survey data only for the period before the contact ban, i.e. using observations from the period March 20 to 22.

quasi steady-state is approached more quickly and the final phase of opening shortly before the vaccination arrives is shortened (Figure 7, top right panel). We also compute optimal dynamics when individual expected present values of an infection would be at the median instead of mean values reported in Table 3, and if we re-calibrate these values assuming $\varepsilon = 0.5$ in the utility function (24), instead of $\epsilon = 0.7$, as in the baseline calibration. The optimal policy is also robust against these alternative specifications (not shown in the figure).

Third, we assume that once a vaccination becomes available the pandemic is stopped (cf. Acemoglu et al., 2020; Farboodi et al., 2020). Hence, we modelled the arrival of a vaccine by a finite time horizon. The timing of the arrival of a vaccine is, however, highly uncertain, with experts expecting a vaccine to become available in between 1 and 2 years Acemoglu et al. (2020). It the vaccine would become available already after one year (52 weeks) instead of two years (104 weeks), the optimal policy response in the beginning of the pandemic and in the quasi-steady state remain largely unchanged (Figure 7, bottom left panel), but obviously the time during which society suppresses the pandemic in the quasi-steady state is reduced.

Finally, we re-calibrate the model considering only a sub-sample of survey respondents (Figure 7, bottom right panel). We turn to this in the next subsection.

5.2 Effects of the contact ban and other distancing policies

During our data collection, the German government announced a nation-wide contact ban on March 22, 2020. This regulation did not allow meeting more than one other person at a time, except for members of the same household, but it did not constrain the total number of daily meetings. This regulation could have affected both the reduction in contacts and the motivation to engage in defense efforts. Table 6 shows the result of the statistical test if there is a difference in the responses collected before and after the introduction of the contact ban. We do not find evidence that the contact ban affected the weights attached to the different reasons for individual protection efforts. This indicates that a crowding out of intrinsic motivation seems unlikely. With regard to the reported change of contacts during the past week, we observe a negative impact: after the contact ban, survey respondents tend to report stronger protection efforts, on average 0.442 points less on the 15-point Likert scale. However, we do not see a clear shift after the contact ban. To the contrary, we observe a continuous downward trend in contacts, as Figure 8 shows.

To study if our main results are affected by the different in social distancing behavior by early and late participants in the survey, we re-calibrate the model using data for the period March 20 to 22 only, ignoring all responses after the contact ban has been in force. This results in mean individual expected present values of an infection of $V_{1t}^i = -5,435$ for young

Figure 8: Reduction of contacts over the data collection period.

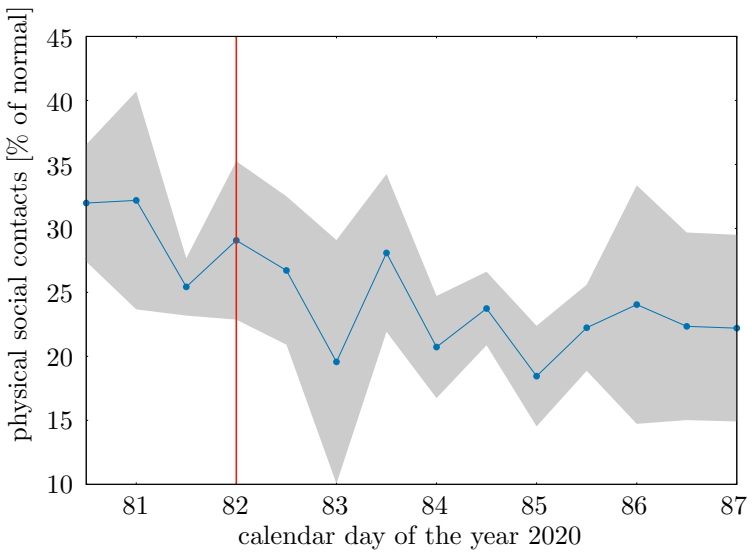

Notes: The graph shows the mean reduction in contacts, measured in percentage reduction from the same week in the last year, grouped by day and daytime (before and after 12pm) of the data collection. The shaded area indicates deviations by two standard errors, and the red line the announcement of the contact ban in the evening of March 22, 2020.

men, $V^i_{2t} = -7,475$ for young women, $V^i_{2t} = -6,208$ for old men and $V^i_{4t} = -8,573$ for old women. The main effect is that the difference in mean values for men and women become more pronounced. Whereas the values for V^i_{jt} for men in the early-respondent subsample are larger (smaller in absolute value) than for the whole sample, the values are smaller (larger in absolute values) for women. Overall the values are similar for both subsamples, however. Accordingly, the socially optimal frequency of physical social contacts is very similar for the re-calibrated model, shown in Figure 7, panel on the bottom right, and for the baseline calibration using the full sample, shown in Figure 3, right panel.

More generally, we consider the 'selfish' part of the individual reduction in the frequency of physical social distancing as the voluntary and unconstrained choice of the individual respondent, resulting in frequencies of contacts between 29.27 and 40.00 percent of normal (cf. Table 4). Our analysis has consistently shown that also in the Nash equilibrium with purely selfish individuals, eventually the epidemic will enter a quasi steady state where individuals choose contacts $\bar{c}_{jt}$ such that their group-specific basic reproduction number would be equal to unity, $\mathcal{R}_{j0} = \beta_0 \, \bar{c}_{jt}/(\mu_j + \alpha_j + \gamma_j) = 1$.[14] We now turn to the question how robust this result is and in particular to what extent it would be changed if the voluntary part of social distancing would be less (or more) than according to our estimates. To this

[14]The corresponding frequencies of physical social contacts, $\bar{c}_{1t} = \bar{c}_{2t} = 32$ percent for young men or women; $\bar{c}_{3t} = 37$ percent for old men, and $\bar{c}_{4t} = 35$ percent for old women, are given in section 4.1.

end, we study how the prevalence of infections, $\overline{I/N}$, at which individuals choose the quasi steady state frequencies of contacts, changes with the input data on the individually optimal number of physical social contacts at the beginning of the epidemic. We use equation (24) that determines the individual expected present value of an infection which must be the same in the assumed quasi steady state during the survey and in the quasi steady state that would result in the laissez-faire Nash equilibrium with purely selfish individuals:

$$\begin{aligned}(1-\delta_j\,(1-\mu_j))\,V_{j0}^i = c_{j0}^{\varepsilon} - \frac{\varepsilon}{1-\varepsilon}\,\left(c_{j0}^{\varepsilon-1}-1\right)\,\frac{1-\delta_j\,(1-\mu_j)}{\delta_j\,\beta_0\,I_0/N_0} \\ = \bar{c}_j^{\varepsilon} - \frac{\varepsilon}{1-\varepsilon}\,\left(\bar{c}_j^{\varepsilon-1}-1\right)\,\frac{1-\delta_j\,(1-\mu_j)}{\delta_j\,\beta_0\,\overline{I/N}}. \quad (25)\end{aligned}$$

From this we obtain the share of infected individuals in quasi steady state in the Nash equilibrium as

$$\overline{I/N} = \frac{(1-\delta_j\,(1-\mu_j))\,\frac{\varepsilon}{1-\varepsilon}\,\left(\bar{c}_j^{\varepsilon-1}-1\right)}{\delta_j\,\beta_0\,\left(\bar{c}_j^{\varepsilon} - c_{j0}^{\varepsilon} + \frac{\varepsilon}{1-\varepsilon}\,\left(c_{j0}^{\varepsilon-1}-1\right)\,\frac{1-\delta_j\,(1-\mu_j)}{\delta_j\,\beta_0\,I_0/N_0}\right)}. \quad (26)$$

Using the epidemiological data reported in table 2, the values for $\bar{c}_j$ reported in footnote 14, and the calibrated preference parameters δ_j and ε, we obtain the results shown in figure 9.

This analysis reveals that the general result is robust over a wide range of alternative input data on physical social contacts at the beginning of the pandemic. Even if the average contacts would have been much higher than our estimates (up to 70% higher for young men, 200% higher for young women), still a quasi steady state at moderate infection levels would result from Nash equilibrium dynamics of selfish individuals. Thus, our results are robust against a large share of regulation-driven contact reductions that may contaminate our interpretation of voluntary behavior.

5.3 Measuring physical distancing using cell-phone data

We furthermore compare the results of our model with observed movements from cell phone data. We use data from the COVID-19 Mobility Project (2020), which provides information on the number of cell phone movements at the county level in Germany. These cell phone movements capture switches in cell phone tower areas for users of the mobile phone providers Telekom and Telefónica, who account for a combined market share of around two-thirds (Bundesnetzagentur, 2020).[15] In contrast to other studies that use mobility data from

[15]While a trip can lead to multiple switches in cell phone tower areas, the data combines multiple switches to a single movements once a person becomes stationary again.

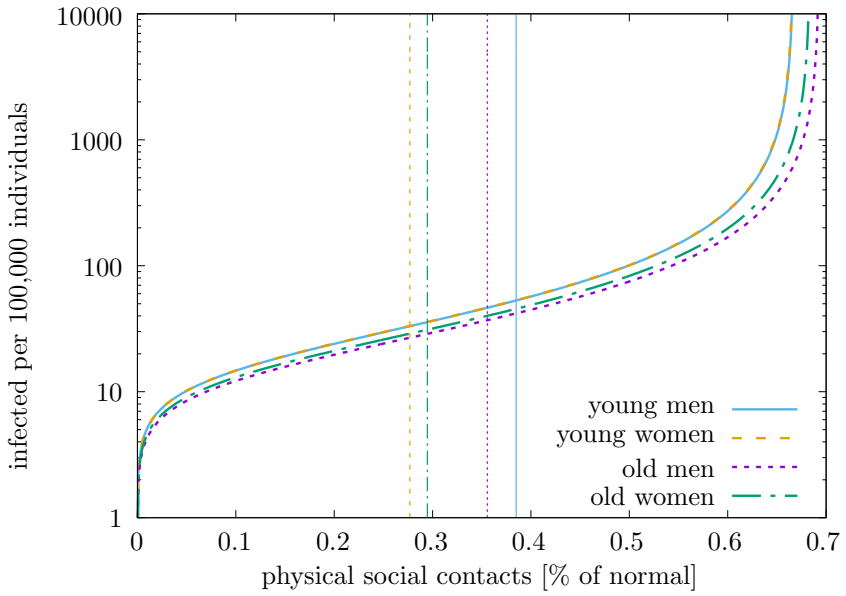

Figure 9: The figure shows how the number of infected individuals in quasi steady state of the Nash equilibrium dynamics would change if the model was not calibrated on the estimated actual number of physical social contacts chosen by selfish individuals at the infection rates prevailing during the time of the survey (shown as vertical lines), but on some other, hypothetical values of c_{j0}.

SafeGraph (Farboodi et al., 2020), Baidu (Kraemer et al., 2020), Apple (Alfaro et al., 2020), or Google, there are two major distinctions to highlight. First, the data we use are retrieved from mobile phone providers. Hence, they capture movements of cell phone users regardless of their installed apps, operating systems, or devices.[16] Second, these cell phone movements reflect the number of trips instead of the number of devices at a specific location, like Point of Interest, or the time spend at home as provided by SafeGraph. While the latter is especially relevant for a US-style *shelter-in-place* policy, the German government introduced a contact ban but did not impose a nationwide curfew. Hence, the actual number of trips is the appropriate data to use for the case of Germany.

Figure 10 shows cell phone movements in 2020 relative to the corresponding weekday in March 2019 over time. We observe are sharp reduction in cell phone movements of 40 to 50 percent starting from the beginning of March, but no clear reduction following the contact ban. During April, however, there is a steady convergence back to previous levels such that there are 20 percent fewer cell phone movements at the beginning of May. The right panel in Figure 10 shows the same data, for the period March 30 to May 6, 2020, plotted over

[16]Individuals in the SafeGraph dataset, for example, need to opt-in and their location data is collected through third-party applications. Similarly, datasets on mobility patterns, as provided by Apple, Google, and Baidu, rely on the users of their navigation applications.

Figure 10: Reduction in cell phone movements in Germany during the COVID-19 spread

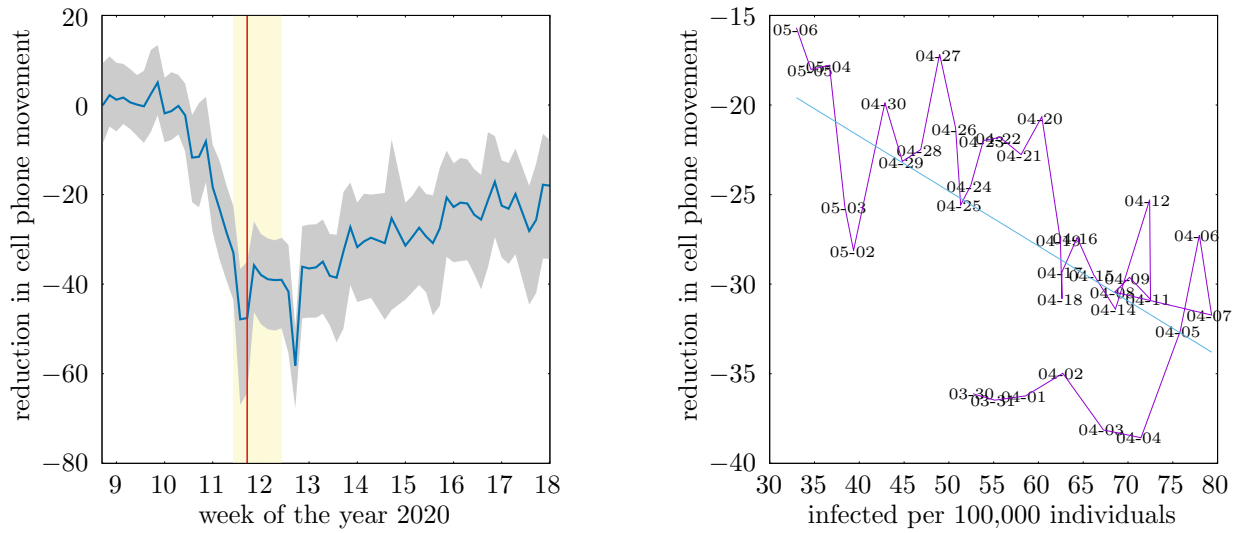

Notes: The graphs show reduction in cell phone movements over the week of the year 2020 relative to the average corresponding weekday in 2019, but excluding public holidays, aggregated to the county level (left panel), and over the fraction of infected, starting on March 30, 2020 (week 13), where estimates of the number of recovered became available. In the left panel, the blue line indicates the median county in Germany, the grey band the 10 – 90 percent interval, and the yellow band the time period of our survey. The red line indicates the announcement of the contact ban. Data is based on COVID-19 Mobility Project (2020), using data from mobile phone providers Telekom and Telefónica. A cell phone movement indicates a switch in cell phone tower areas after a person becomes stationary again.

the estimated number of COVID-19 infections. Consistent with the model, cf. (9), there is a negative correlation between the reduction of cell phone movements, as a proxy for the reduction in the number of physical social contacts, and the number of infected individual.

5.4 Discussion of potential extensions

As any model analysis, ours abstracts from a number of potentially interesting issues. In the following, we discuss potential extensions of the analysis and the likely effects on results, based on the existing literature.

We do not consider limits to the health care system and thus a 'health care externality' in addition to the infection externality (see, e.g., Farboodi et al., 2020; Bethune and Korinek, 2020), as it does not seem to be of practical relevance for our German case study. Yet, in principle, the model could be readily extended along these lines by making transition rates γ_j, and α_j dependent on I_t. This would likely have the effect that the social cost of an elderly infection will rise, due to longer stay in hospitals. For instance, Farboodi et al. (2020) find that considering in addition to the infection externality also a health care externality, i.e.

that the quality of health care decreases as more individuals get infected due to capacity constraints and congestion of the health care system, leads to an even stronger 'flattening of the curve' in the social optimum.

Secondly, we did not consider issues of detecting infectious individuals and optimal testing. To do so, one would extend our HetSIR model to include a state in which individuals are infectious, but show no or only light symptoms. Such a model could be used to study optimal population group-specific testing (with imperfectly altruistic preferences) in a situation where testing is costly with increasing marginal costs. For instance, Brotherhood et al. (2020) augment the SIR model to include an additional health state at which individuals show symptoms, but uncertainty about whether they have COVID-19 or a common flu only resolves after some time. In their model testing reduces this time of uncertainty.

Third, the HetSIR model used here can facilitate any number of population groups and our empirical analysis can also be extended accordingly. For instance one could consider age classes of 10-years, distinguish by income or pre-existing illnesses. We have limited our analysis to four population groups (distinguished by age and gender) that show significant differences in their contact reductions and in other key characteristics in our German case study for expositional purposes. As the virological literature on more fine-grained differences across population groups is still in flux, such extensions would be worthwhile retrospectively when sufficient clarity has been achieved.

Finally, we have taken a standard Utilitarian welfare function as the social objective, thereby following a widespread approach in both economics and moral philosophy. However, it would be interesting to compare this to alternative objectives, such as Prioritarianism (Adler et al., 2019), or approaches that specifically value individual freedom of movement or choice of contacts, for instance.

6 Conclusion

Drawing on the epidemiological SIR model we have developed an economic-epidemiological model (HetSIR) with forward-looking heterogeneous individuals susceptible to virus infection. Imperfectly altruistic subjects choose their number of contacts balancing current utility from physical social contacts with the expected present value of the infection risk. We have characterized private behavior of individuals susceptible to a virus infection, and socially optimal social distancing. We have quantified the model with unique data on social distancing behavior and impure altruistic motivations from a large, representative survey among around 3,500 Germans conducted at the beginning of the COVID-19 epidemic, and we have calibrated our model to official epidemiological data.

We find that the optimal policy reduces contacts drastically in the beginning of the pandemic to virtually eradicate the virus and to stabilize the spread at a quasi-steady state until a vaccine becomes tangible. Moreover, we find a substantial gap between private and social costs of contacts. Specifically, we find that the social costs of an infection are around 5 times higher than the private costs at the selfish Nash equilibrium, and more than 25 times higher at the socially-optimal level of infected for the main part of the pandemic. Pure selfish behavior does not lead to such a drastic initial reduction in contacts, but also reaches a quasi-steady state at infection levels of around 10 infected per 100,000 individuals. This is very moderate compared to a potential peak without behavioral adjustments, but far higher than in the social optimum. Whereas all socio-demographic groups should and do reduce physical social contacts to roughly similar extents, our results suggests a tendency that more severely affected groups need to be constrained less, as they tend to impose less of a risk on others in case they get infected. Moreover, the impure altruistic behavior of our respondents closes around a third of the gap between the selfish 'laissez-faire' and socially optimal contact reductions. This contributes new evidence to a long-standing literature by pointing towards an important role of impure altruism for the private provision of a public good—in a setting in which both the externality and the number of people profiting from an externality reduction is very large (e.g. Andreoni, 1988, 1990, 2007; Goeree et al., 2002; Ottoni-Wilhelm et al., 2017).

Overall, we show that while there is a sizable gap between the private and social cost of contacts, private actions for self-protection and for the protection of others can contribute substantially toward alleviating the problem of social cost. Our paper thus also contributes a high-stakes case study to the literature on the private provision of a public good under uncertainty (e.g. Barrett and Dannenberg, 2014; Bramoullé and Treich, 2009; McBride, 2006; Tavoni et al., 2011; Quaas and Baumgärtner, 2008).

Naturally, our study is subject to a number of limitations. First, our survey responses on contact reductions are based on reported rather than observed behavior. The comparison with contacts based on cell-phone data showed, however, that both approaches of observing social distancing behavior were by and large consistent. Moreover, stated contact reductions can contain effects of milder regulations before the contact ban came in place via reduced contact opportunities, such as the cancellation of large-scale events. Our survey data reveal that the majority of respondents in all groups reduce contacts more than as was prescribed. Thus, while it seems elusive to cleanly disentangle voluntary action from reactions to regulations, our interpretation of the selfish Nash equilibrium may be too optimistic concerning what private actions can achieve in containing the pandemic. Our analysis, however, reveals that our results are qualitatively robust to considerable misinterpretations of this kind.

Second, we have not explicitly studied income losses due to social distancing in the pandemic. Rather, we have assumed that individuals factor in their contact-dependent income losses as part of their internal calculation on contact reduction, as our survey question did not distinguish between work or leisure related contacts. Future work should include utility depending on health status, (social) contacts and income that derives from work contacts, and examine how production depends on contacts, and to what degree jobs can be performed remotely (e.g. Dingel and Neiman, 2020; Fadinger and Schymik, 2020).

Finally, we have assumed that the marginal utility of physical social contacts is decreasing, implying that some types of social contacts are more important than others. However, while individuals have a priority order of contacts and would choose their contracts differently from what governments prescribe, there is an additional value loss from contact bans as compared to voluntary choice. As our data do not disentangle different kinds of contacts, we are not able to offer recommendations on which types of contacts should be prohibited or allowed, and can also not speak to potential 'social contact-budget' mechanisms, such as individually transferable quotas for contacts or liability rules.

In the context of the COVID-19 pandemic, our results imply that the 'flattening of the curve' observed in several Western societies, and in Germany in particular, may be explained as a Nash equilibrium outcome and not necessarily as a particular success of policy intervention. While we can attribute the bulk of observed contact reductions to voluntary behavior—in line with evidence for COVID-19, for instance, by Yan et al. (2020) and for the A/H1N1 swine flu by Bayham et al. (2015)— this certainly does not imply that governmental actions are superfluous. Even without strict contact regulations, public actors can play important roles in appealing to social norms and in making the risks of infection salient. Nevertheless, our results show that the social cost of contacts is up to orders of magnitude larger than the private cost. Thus, given the size of the externality, there is indeed *"no reason why [...] governmental administrative regulation should not lead to an improvement in economic efficiency"*, as Coase (1960, p.18) put it in his problem of social cost. We show that decisive governmental action is, in particular, crucial to contain the virus directly at the beginning of a pandemic to reduce the number of fatalities.

Acknowledgements

We are grateful to Adam Clark and Eli Fenichel for helpful comments, to Alexander Mahler and Fabian Marder for research assistance, and to Dr. med. Nils Kellner for supporting the survey. We acknowledge funding by the German Federal Ministry of Education and Research (BMBF) under grant number 01LC1826E.

References

Acemoglu, D., Chernozhukov, V., Werning, I., Whinston, M.D., 2020. A Multi-Risk SIR Model with Optimally Targeted Lockdown. Working Paper 27102. National Bureau of Economic Research. Cambridge.

Adler, M.D., Ferranna, M., Hammitt, J.K., Treich, N., 2019. Fair innings: The utilitarian and prioritarian value of risk reduction over a whole lifetime. SSRN WP 3493976 .

Alfaro, L., Faia, E., Lamersdorf, N., Saidi, F., 2020. Social Interactions in Pandemics: Fear, Altruism, and Reciprocity. Working Paper 27134. National Bureau of Economic Research. Cambridge.

Alvarez, F.E., Argente, D., Lippi, F., 2020. A simple planning problem for covid-19 lockdown. Working Paper 26981. National Bureau of Economic Research. Cambridge.

Andreoni, J., 1988. Privately provided public goods in a large economy: the limits of altruism. Journal of Public Economics 35, 57–73.

Andreoni, J., 1990. Impure altruism and donations to public goods: A theory of warm-glow giving. The Economic Journal 100, 464–477.

Andreoni, J., 2007. Giving gifts to groups: How altruism depends on the number of recipients. Journal of Public Economics 91, 1731–1749.

Andreoni, J., Sprenger, C., 2012. Estimating time preferences from convex budgets. American Economic Review 102, 3333–56.

Attema, A.E., Bleichrodt, H., Gao, Y., Huang, Z., Wakker, P.P., 2016. Measuring discounting without measuring utility. American Economic Review 106, 1476–94.

Avery, C., Bossert, W., Clark, A., Ellison, G., Ellison, S.F., 2020. Policy Implications of Models of the Spread of Coronavirus: Perspectives and Opportunities for Economists. Working Paper 27007. National Bureau of Economic Research. Cambridge. doi:10.3386/w27007.

Barrett, S., 2003. Global disease eradication. Journal of the European Economic Association 1, 591–600.

Barrett, S., Dannenberg, A., 2014. Sensitivity of collective action to uncertainty about climate tipping points. Nature Climate Change 4, 36–39.

Barrett, S., Hoel, M., 2007. Optimal disease eradication. Environment and Development Economics 12, 627–652.

Baud, D., Qi, X., Nielsen-Saines, K., Musso, D., Pomar, L., Favre, G., 2020. Real estimates of mortality following covid-19 infection. The Lancet infectious diseases .

Bayham, J., Kuminoff, N.V., Gunn, Q., Fenichel, E.P., 2015. Measured voluntary avoidance behaviour during the 2009 a/h1n1 epidemic. Proceedings of the Royal Society B: Biological Sciences 282, 20150814.

Bethune, Z.A., Korinek, A., 2020. Covid-19 Infection Externalities: Trading Off Lives vs. Livelihoods. Working Paper 27009. National Bureau of Economic Research. Cambridge.

Bodenstein, M., Corsetti, G., Guerrieri, L., 2020. Social Distancing and Supply Disruptions in a Pandemic. Working Paper 2020-031. Board of Governors of the Federal Reserve System. Washington.

Boldog, P., Tekeli, T., Vizi, Z., Dénes, A., Bartha, F., Röst, G., 2020. Risk assessment of novel coronavirus covid-19 outbreaks outside China. Journal of Clinical Medicine 9, 571.

Bos, B., Drupp, M.A., Meya, J.N., Quaas, M.F., 2020. Expectations and private defense measures in the covid pandemic. Unpublished manuscript.

Bramoullé, Y., Treich, N., 2009. Can uncertainty alleviate the commons problem? Journal of the European Economic Association 7, 1042–1067.

Brotherhood, L., Kircher, P., Santos, C., Tertilt, M., 2020. An economic model of the Covid-19 epidemic: The importance of testing and age-specific policies. Discussion Paper 14695. Centre for Economic Policy Research. London.

Bundesnetzagentur, 2020. Teilnehmerentwicklung im mobilfunk. URL: `https://www.bundesnetzagentur.de/DE/Sachgebiete/Telekommunikation/Unternehmen_Institutionen/Marktbeobachtung/Deutschland/Mobilfunkteilnehmer/Mobilfunkteilnehmer_node.html`. Access on May 12, 2020.

Byrd, R., Hribar, M., Nocedal, J., 1999. An interior point method for large scale nonlinear programming. SIAM Journal of Optimization 9, 877–900.

Byrd, R., Nocedal, J., Waltz, R., 2006. Knitro: An integrated package for nonlinear optimization, in: di Pillo, G., Roma, M. (Eds.), Large-Scale Nonlinear Optimization. Springer, New York, NY, p. 35–59.

Chudik, A., Pesaran, M.H., Rebucci, A., 2020. Voluntary and Mandatory Social Distancing: Evidence on COVID-19 Exposure Rates from Chinese Provinces and Selected Countries. Working Paper 8243. CESifo. Munich.

Coase, R.H., 1960. The problem of social cost. Journal of Law and Economics 3, 1–44.

Cohen, J.D., Ericson, K., Laibson, D., White, J.M., 2020. Measuring time preferences. Journal of Economic Literature, forthcoming.

Coibion, O., Gorodnichenko, Y., Weber, M., 2020. The Cost of the COVID-19 Crisis: Lockdowns, Macroeconomic Expectations, and Consumer Spending. Working Paper 27141. National Bureau of Economic Research. Cambridge.

COVID-19 Mobility Project, 2020. Mobility monitor. URL: `https://www.covid-19-mobility.org/mobility-monitor/`.

Dasaratha, K., 2020. Virus dynamics with behavioral responses. URL: `https://arxiv.org/abs/2004.14533v1`. Unpublished manuscript.

Dingel, J.I., Neiman, B., 2020. How many jobs can be done at home? Working Paper 26948. National Bureau of Economic Research. Cambridge.

Dohmen, T., Falk, A., Huffman, D., Sunde, U., 2010. Are risk aversion and impatience related to cognitive ability? American Economic Review 100, 1238–60.

Dorigatti, I., Okell, L., Cori, A., Imai, N., Baguelin, M., Bhatia, S., Boonyasiri, A., Cucunubá, Z., Cuomo-Dannenburg, G., FitzJohn, R., et al., 2020. Report 4: severity of 2019-novel coronavirus (ncov). Imperial College London, London .

Dowd, J.B., Andriano, L., Brazel, D.M., Rotondi, V., Block, P., Ding, X., Liu, Y., Mills, M.C., 2020. Demographic science aids in understanding the spread and fatality rates of covid-19. Proceedings of the National Academy of Sciences .

Drupp, M.A., Freeman, M.C., Groom, B., Nesje, F., 2018. Discounting disentangled. American Economic Journal: Economic Policy 10, 109–134.

Eichenbaum, M.S., Rebelo, S., Trabandt, M., 2020. The macroeconomics of epidemics. Working Paper 26882. National Bureau of Economic Research. Cambridge.

Fadinger, H., Schymik, J., 2020. The costs and benefits of home office during the covid-19 pandemic: Evidence from infections and an input-output model for germany. COVID Economics: Vetted and Real-Time Papers 9, 107–134.

Falk, A., Becker, A., Dohmen, T., Enke, B., Huffman, D., Sunde, U., 2018. Global evidence on economic preferences. The Quarterly Journal of Economics 133, 1645–1692.

Famulare, M., 2020. 2019-ncov: preliminary estimates of the confirmed-case-fatality-ratio and infection-fatality-ratio, and initial pandemic risk assessment. URL: https://institutefordiseasemodeling.github.io/nCoV-public/analyses/first_adjusted_mortality_estimates_and_risk_assessment/2019-nCoV-preliminary_age_and_time_adjusted_mortality_rates_and_pandemic_risk_assessment.html.

Farboodi, M., Jarosch, G., Shimer, R., 2020. Internal and External Effects of Social Distancing in a Pandemic. Working Paper 27059. National Bureau of Economic Research. Cambridge.

Federal Statistical Office Germany, 2020. Life table (period life table): Germany, period of years, sex, completed age. [Code 12621-0001]. URL: https://www-genesis.destatis.de/genesis//online?operation=table&code=12621-0001&levelindex=0&levelid=1589551040818. Accessed on May, 15, 2020.

Fenichel, E.P., 2013. Economic considerations for social distancing and behavioral based policies during an epidemic. Journal of Health Economics 32, 440–451.

Fenichel, E.P., Castillo-Chavez, C., Ceddia, M.G., Chowell, G., Parra, P.A.G., Hickling, G.J., Holloway, G., Horan, R., Morin, B., Perrings, C., Springborn, M., Velazquez, L., Villalobos, C., 2011. Adaptive human behavior in epidemiological models. Proceedings of the National Academy of Sciences 108, 6306–6311.

Ferretti, L., Wymant, C., Kendall, M., Zhao, L., Nurtay, A., Abeler-Dörner, L., Parker, M., Bonsall, D., Fraser, C., 2020. Quantifying sars-cov-2 transmission suggests epidemic control with digital contact tracing. Science 368.

Gerlagh, R., 2020. Closed-form solutions for optimal social distancing in a SIR model of covid-19 suppression. URL: https://surfdrive.surf.nl/files/index.php/s/urD08aZYqCIvnI9. Unpublished manuscript.

Gersovitz, M., 2011. The economics of infection control. Annual Review of Resource Economics 3, 277–296.

Gersovitz, M., Hammer, J.S., 2004. The economical control of infectious diseases. The Economic Journal 114, 1–27.

Goeree, J.K., Holt, C.A., Laury, S.K., 2002. Private costs and public benefits: unraveling the effects of altruism and noisy behavior. Journal of Public Economics 83, 255–276.

Gollier, C., 2020. Cost-benefit analysis of age-specific deconfinement strategies. URL: https://drive.google.com/file/d/1Hs7VBjQC9OWn1a_vEyaTExf97uORKBId/view. Unpublished manuscript.

Gonzalez-Eiras, M., Niepelt, D., 2020. On the Optimal "Lockdown" During an Epidemic. Working Paper 8240. CESifo. Munich.

Greenstone, M., Nigam, V., 2020. Does Social Distancing Matter? Working Paper 2020-26. University of Chicago, Becker Friedman Institute for Economics Working Paper. Chicago.

Greenwood, J., Kircher, P., Santos, C., Tertilt, M., 2019. An equilibrium model of the african HIV/AIDS epidemic. Econometrica 87, 1081–1113.

Grimm, V., Mengel, F., Schmidt, M., 2020. Extensions of the SEIR model for the analysis of tailored social distancing and tracing approaches to cope with covid-19. URL: http://www.wirtschaftstheorie.wiso.uni-erlangen.de/wp-content/uploads/2020/04/Grimm_Mengel_Schmidt__2020.pdf. Unpublished manuscript.

Guerrieri, V., Lorenzoni, G., Straub, L., Werning, I., 2020. Macroeconomic Implications of COVID-19: Can Negative Supply Shocks Cause Demand Shortages? Working Paper 26918. National Bureau of Economic Research. Cambridge.

Harrison, G., Lau, M., Williams, M., 2002. Estimating individual discount rates in denmark: A field experiment. American Economic Review 92, 1606–1617.

Harsanyi, J., 1955. Cardinal welfare, individualistic ethics and interpersonal comparisons of utility. Journal of Political Economy 63, 309–321.

He, X., Lau, E.H., Wu, P., Deng, X., Wang, J., Hao, X., Lau, Y.C., Wong, J.Y., Guan, Y., Tan, X., et al., 2020. Temporal dynamics in viral shedding and transmissibility of covid-19. Nature Medicine 26, 672–675.

an der Heiden, M., Buchholz, U., 2020. Modellierung von Beispielszenarien der SARS-CoV-2-Epidemie 2020 in Deutschland. Robert Koch Institut.

Jones, C.J., Philippon, T., Venkateswaran, V., 2020. Optimal mitigation policies in a pandemic: Social distancing and working from home. Working Paper 26984. National Bureau of Economic Research. Cambridge.

Kermack, W.O., McKendrick, A.G., 1927. A contribution to the mathematical theory of epidemics. Proceedings of the royal society of london. Series A, Containing papers of a mathematical and physical character 115, 700–721.

Kraemer, M.U.G., Yang, C.H., Gutierrez, B., Wu, C.H., Klein, B., Pigott, D.M., Group†, O.C..D.W., Plessis, L.d., Faria, N.R., Li, R., Hanage, W.P., Brownstein, J.S., Layan, M., Vespignani, A., Tian, H., Dye, C., Pybus, O.G., Scarpino, S.V., 2020. The effect of human mobility and control measures on the COVID-19 epidemic in China. Science 368, 493–497.

Li, L.q., Huang, T., Wang, Y.q., Wang, Z.p., Liang, Y., Huang, T.b., Zhang, H.y., Sun, W., Wang, Y., 2020. Covid-19 patients' clinical characteristics, discharge rate, and fatality rate of meta-analysis. Journal of medical virology 92, 577–583.

Maier, B.F., Brockmann, D., 2020. Effective containment explains subexponential growth in recent confirmed covid-19 cases in china. Science 368, 742–746.

McBride, M., 2006. Discrete public goods under threshold uncertainty. Journal of Public Economics 90, 1181–1199.

Morin, B.R., Fenichel, E.P., Castillo-Chaves, C., 2013. SIR dynamics with economically driven contact rates. Natural Resource Modeling 26, 505–525.

Ottoni-Wilhelm, M., Vesterlund, L., Xie, H., 2017. Why do people give? testing pure and impure altruism. American Economic Review 107, 3617–33.

Pindyck, R.S., 2020. COVID-19 and the welfare effects of reducing contagion. Working Paper 27121. National Bureau of Economic Research. Cambridge.

Pinotti, F., Di Domenico, L., Ortega, E., Mancastroppa, M., Pullano, G., Valdano, E., Boelle, P.Y., Poletto, C., Colizza, V., 2020. Lessons learnt from 288 covid-19 international cases: importations over time, effect of interventions, underdetection of imported cases. URL: `https://www.medrxiv.org/content/10.1101/2020.02.24.20027326v1.full.pdf`. Unpublished manuscript.

Quaas, M.F., Baumgärtner, S., 2008. Natural vs. financial insurance in the management of public-good ecosystems. Ecological Economics 65, 397–406.

Rachel, L., 2020. An analytical model of covid-19 lockdowns. URL: `https://drive.google.com/file/d/1tVTfyEeD0xTIcZVlvCZvDN95CZ6uVdmU/view`. Unpublished manuscript.

Read, J.M., Bridgen, J.R., Cummings, D.A., Ho, A., Jewell, C.P., 2020. Novel coronavirus 2019-ncov: early estimation of epidemiological parameters and epidemic predictions. URL: https://www.medrxiv.org/content/10.1101/2020.01.23.20018549v2. Unpublished manuscript.

Robert Koch Institut, 2020a. Daily situation reports. URL: https://www.rki.de/DE/Content/InfAZ/N/Neuartiges_Coronavirus/Situationsberichte/Gesamt.html. Accessed on May 5, 2020.

Robert Koch Institut, 2020b. Fallzahlen in Deutschland. URL: https://npgeo-corona-npgeo-de.hub.arcgis.com/datasets/dd4580c810204019a7b8eb3e0b329dd6_0. Accessed on April, 30, 2020.

Rocklöv, J., Sjödin, H., Wilder-Smith, A., 2020. Covid-19 outbreak on the diamond princess cruise ship: estimating the epidemic potential and effectiveness of public health countermeasures. Journal of Travel Medicine, forthcomming.

Roemer, J.E., 1996. Theories of Distributive Justice. Harvard University Press, Cambridge, Massachusetts.

Rothe, C., Schunk, M., Sothmann, P., Bretzel, G., Froeschl, G., Wallrauch, C., Zimmer, T., Thiel, V., Janke, C., Guggemos, W., et al., 2020. Transmission of 2019-ncov infection from an asymptomatic contact in germany. New England Journal of Medicine 382, 970–971.

Rowthorn, B.R., Toxvaerd, F., 2012. The optimal control of infectious diseases via prevention and treatment. Discussion Paper 8925. Centre for Economic Policy Research. London.

Tavoni, A., Dannenberg, A., Kallis, G., Löschel, A., 2011. Inequality, communication, and the avoidance of disastrous climate change in a public goods game. Proceedings of the National Academy of Sciences 108, 11825–11829.

Toxvaerd, F., 2020. Equilibrium Social Distancing. Working Paper 2021. Faculty of Economics. Cambridge.

Verity, R., Okell, L.C., Dorigatti, I., Winskill, P., Whittaker, C., Imai, N., Cuomo-Dannenburg, G., Thompson, H., Walker, P.G., Fu, H., et al., 2020. Estimates of the severity of coronavirus disease 2019: a model-based analysis. The Lancet Infectious Diseases, forthcomming.

Yan, Y., Malik, A.A., Bayham, J., Fenichel, E.P., Couzens, C., Omer, S.B., 2020. Measuring voluntary social distancing behavior during the covid-19 pandemic. URL: https://www.medrxiv.org/content/10.1101/2020.05.01.20087874v1. Unpublished manuscript.

Appendix

Table 5: Summary statistics of the survey data.

	N	Mean	Median	Std. Dev.	Min.	Max.
Change in contacts	3495	4.81	4	3.48	1	15
Age	3501	50.05	51	15.40	18	97
Female	3501	0.51	1	0.50	0	1
Family members and friends	3495	14.10	10	13.02	0	100
Reason for defense efforts (in %)						
To protect me	3499	51.96	50	21.75	0	100
To protect family & friends	3499	30.03	30	15.90	0	100
To protect others	3499	18.01	20	14.37	0	100
Expectations						
Expected income change	3494	6.98	8	2.41	1	15
P(get infected) (in %)	3486	38.10	40	22.40	0	100
P(get slightly ill) (in %)	3404	50.65	50	21.71	0	100
P(get in acute danger) (in %)	3404	34.65	30	20.88	0	100
Change wrt. regulation (in %)						
According to regulations	3501	0.30	0	0.46	0	1
Less than required	3501	0.07	0	0.26	0	1
More than required	3501	0.63	1	0.48	0	1
General preferences						
Patience	3499	8.11	9	2.12	1	11
Observations	3501					

Table 6: Effects of the contact ban announcement.

	Motivation			Contacts			
	Protect me	Protect family & friends	Protect others	Past week	Less than required	As required	More than required
	(1)	(2)	(3)	(4)	(5)	(6)	(7)
Post ban announcement	0.976	-0.875	-0.101	-0.442***	-0.016	0.086***	-0.070***
	(0.825)	(0.613)	(0.570)	(0.138)	(0.012)	(0.018)	(0.019)
Age	0.218***	-0.107***	-0.110***	-0.012**	-0.002***	-0.003***	0.005***
	(0.028)	(0.021)	(0.020)	(0.005)	(0.000)	(0.001)	(0.001)
Female	0.961	0.697	-1.658***	-0.966***	-0.054***	-0.027	0.081***
	(0.839)	(0.625)	(0.582)	(0.137)	(0.012)	(0.018)	(0.019)
Education							
University degree	-2.277	10.760*	-8.483	0.909	0.061	-0.018	-0.043
	(4.506)	(6.460)	(6.026)	(1.682)	(0.068)	(0.155)	(0.167)
A-levels/ vocational training	-2.650	11.943*	-9.292	0.840	0.037	-0.051	0.015
	(4.478)	(6.449)	(6.007)	(1.682)	(0.068)	(0.155)	(0.167)
Secondary school	1.460	10.378	-11.838**	0.819	0.052	-0.054	0.002
	(4.442)	(6.435)	(5.987)	(1.679)	(0.068)	(0.154)	(0.167)
Secondary general school	0.473	10.688*	-11.161*	1.114	0.045	-0.032	-0.013
	(4.474)	(6.443)	(5.988)	(1.682)	(0.068)	(0.154)	(0.167)
Household income							
1,500 – 3,000	0.000	0.579	-0.579	0.013	-0.043**	-0.008	0.051*
	(1.203)	(0.879)	(0.771)	(0.201)	(0.019)	(0.027)	(0.028)
3,000 - 4,000	-0.940	1.044	-0.104	-0.277	-0.081***	-0.027	0.107***
	(1.286)	(0.949)	(0.877)	(0.221)	(0.019)	(0.030)	(0.031)
$\geq$ 4,000	0.350	0.201	-0.551	-0.624***	-0.057***	-0.070**	0.127***
	(1.433)	(1.040)	(0.949)	(0.233)	(0.021)	(0.031)	(0.033)
Observations	3481	3481	3481	3478	3483	3483	3483

Notes: OLS estimations for a weighted sample. Respondents before the ban are reweighted to match the mean values in age, gender, education, and income of those after the ban. Standard errors in parentheses. * $p < 0.1$, ** $p < 0.05$, *** $p < 0.01$

Figure 11: Correlation between survey responses and cell phone movements.

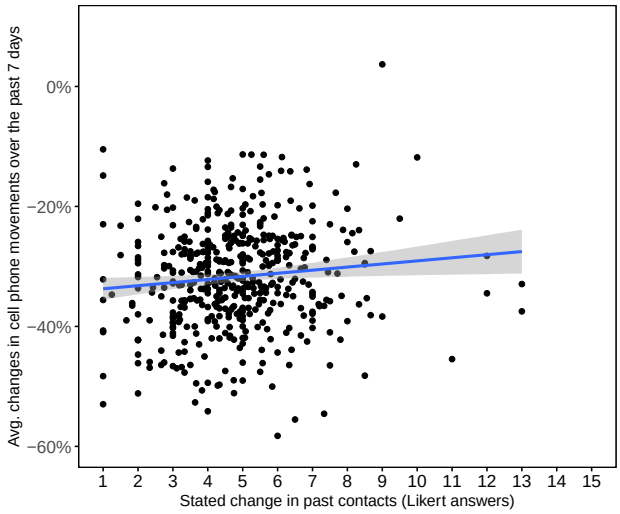

Notes: Plot shows the correlation between the average survey responses and reductions in cell phone movements per county.

Numerical approach and AMPL programming code

Numerically, the problem to solve the set of dynamic equations that describe epidemiological dynamics, and the optimality conditions, (1), (11a), (11b), and (13), along with initial conditions for the number of susceptibles, infected, and recovered from all groups of individuals, and transversality conditions, is usually a more difficult task than solving an optimization problem. In our approach to compute the utilitarian optimum, we thus use the following corollary to Proposition 4:

Corollary 1. *If $\mu_j = 0$ for all j, the social optimization problem* (10) *is equivalent to*

$$\hat{W} = \max_{\{c_{jt}\}} \sum_j \sum_{t=0}^{T} \delta_j^t \left(S_{jt}\, u_j^s(c_{jt}) + I_{jt}\, V_{jt}^i \right) \quad \textit{subject to } (1), \tag{27}$$

where individual present values of becoming infected, V_{jt}^i, is given by (6)*.*

Proof. The optimality conditions for (27) can be written as

$$u_j^{s\prime}(c_{jt}^\star) + \delta_j\, \beta'(c_{jt}^\star)\, \frac{I_t}{N_t} \left(\lambda_{jt}^i - \lambda_{jt}^s \right) = 0 \tag{28a}$$

$$u_j^s(c_{jt}^\star) - \lambda_{j,t-1}^s + \delta_j\, \lambda_{jt}^s + \delta_j\, \beta(c_{jt}^\star)\, \frac{I_t}{N_t} \left(\lambda_{jt}^i - \lambda_{jt}^s \right) = 0 \tag{28b}$$

$$V_{jt}^i - \lambda_{j,t-1}^i + \delta_j\, (1 - \alpha_j - \gamma_j) \lambda_{jt}^i = \sum_l \delta_l\, \beta(c_{lt}^\star)\, \frac{S_{lt}}{N_t} \left(\lambda_{lt}^s - \lambda_{lt}^i \right) \tag{28c}$$

$$-\lambda_{j,t-1}^r + \delta_j\, \lambda_{jt}^r = 0 \tag{28d}$$

$$-\lambda_{j,t-1}^d + \delta_j\, \lambda_{jt}^d = 0, \tag{28e}$$

with transversality conditions $\lambda_{jT}^h = V_j^n$ for all $h \in \{s, i\}$ and $\lambda_{jT}^h = 0$ for $h \in \{r, d\}$. We can ignore (28d) and (28e), as neither λ_{jt}^r nor λ_{jt}^d affect $c_{jt}^\star$. Equations (28a) and (28b) are identical to (11a) and (11b). Equation (28c) is equivalent to (13). □

In the following we provide the AMPL code for computing the utilitarian optimal epidemiological dynamics, as shown in Figure 3. The codes used for computing the results for the other figures are all based on this code and are available upon request.

run file "EconEpi.run", call with "ampl EconEpi.run"

```
  reset;
model EpiEcon.mod;
data EpiEcon.dat;

option solver "knitroampl"; # use Knitro to solve the nonlinear optimization problem
option knitro_options "feastol 10e-13 xtol 10e-13";

let {j in 1..n} delta[j] := 0.9; # set discount factors at rather low values, to obtain an initial
guess for the optimal solution
solve; # compute optimal solution

option knitro_options "xtol 10e-13 algorithm 3"; # change to other optimization algorithm

let {j in 1..n} delta[j] := 0.95; # increase discount factor to the calibrated level
solve;
let {j in 1..n} delta[j] := 0.99;
solve;
let {j in 1..n} delta[j] := 0.995; # here we are
solve; # final solution

# write output to file "out.csv"
for {t in 0..T} {
printf "%d\t", t >out.csv; # current week
printf {j in 1..n} "%f\t", 100*c[j,t]>out.csv; # physical social contacts in percent of normal
printf {j in 1..n} "%f\t", 100000*I[j,t]>out.csv; # infected per 100,000 individuals
printf {j in 1..n} "%f\t", infected[j,t]>out.csv; # lamdba_j^i
printf "\n">out.csv; # new line
}
```

model file "EconEpi.mod"

```
   param T; # time horizon
param n; # number of groups
param delta {j in 1..n}; # discount factor
param mu {j in 1..n}; # baseline mortality
param alpha {j in 1..n}; # COVID mortality
param gamma {j in 1..n}; # recovery rate
param beta0 {j in 1..n}; # baseline transmission rate
param epsilon; # parameter of utility function
param Viinf {j in 1..n}; # individual expected present value of an infection, infinite time horizon
param Vi {j in 1..n, t in 0..T+1}=(1-(delta[j]*(1-mu[j]-alpha[j]-gamma[j])^(T-t+1)))*Viinf[j];
# individual expected present value of an infection, finite time horizon
param I0 {j in 1..n}; # initial fraction of infected
param S0 {j in 1..n}; # initial fraction of susceptible

var S {j in 1..n, t in 0..T+1}>=0; # susceptible
var I {j in 1..n, t in 0..T+1}>=0; # infected
var R {j in 1..n, t in 0..T+1}>=0; # recovered
var N {t in 0..T+1}=sum {j in 1..n} (S[j,t]+I[j,t]+R[j,t]); # total alive
var c {j in 1..n, t in 0..T}>= 0 <= 1; # physical social contacts

maximize utilitarian: sum {j in 1..n, t in 0..T} (delta[j]^(t)*(S[j,t]*(epsilon/(1-epsilon))*(
(1/epsilon)*c[j,t]^(epsilon)-c[j,t])+I[j,t]*Vi[j,t])); # objective, as characterized in Corollary 1

# epidemiological dynamics
subject to susceptible {j in 1..n, t in 0..T}: S[j,t+1]=(1-mu[j])*S[j,t]-beta0[j]*c[j,t]*(sum {l
in 1..n} I[l,t])/N[t]*S[j,t];
subject to infected {j in 1..n, t in 0..T}: I[j,t+1]=(1-mu[j]-alpha[j]-gamma[j])*I[j,t]+beta0[j]*c[j,t]*(sum
{l in 1..n} I[l,t])/N[t]*S[j,t];
subject to recovered {j in 1..n, t in 0..T}: R[j,t+1]=(1-mu[j])*R[j,t]+gamma[j]*I[j,t];

# initial conditions
subject to initialS {j in 1..n}: S[j,0]=S0[j]-I0[j];
subject to initialI {j in 1..n}: I[j,0]=I0[j];
subject to initialR {j in 1..n}: R[j,0]=0;
```

model file "EconEpi.dat" param T:=104; # weeks

param mu:=
1 0.000028
2 0.000016
3 0.000844
4 0.000721;

param alpha:=
1 0.00285
2 0.000863
3 0.125
4 0.0849;

param n:=4; # ym, yf, om, of

param beta0:=
1 2.16
2 2.16
3 2.16
4 2.16;

param gamma:=
1 0.689
2 0.689
3 0.689
4 0.680;

param epsilon:=0.7;

param Viinf:=
1 -5780
2 -7117
3 -6360

4 -7522;

param I0:=
1 0.00013138
2 0.0001056
3 0.00002957
4 0.00002219;

param S0:=
1 0.3248
2 0.3748
3 0.1602
4 0.1402;